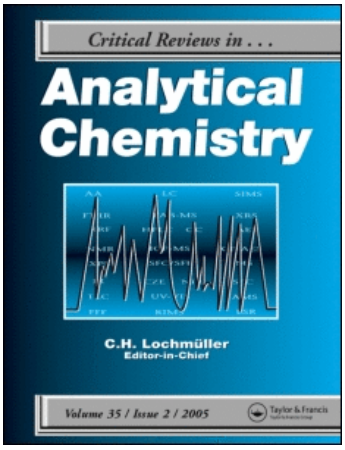

Critical Reviews in Analytical Chemistry
Publication details, including instructions for authors and subscription information:
http://www.informaworld.com/smpp/title~content=t713400837

Electrolytic Chromatography and Coulopotentiography - A Rapid Electrolysis at the Column Electrode used for the Preparation, Separation, Concentration, and Estimation of Trace and/or Unstable Substances

Taitiro Fujinaga; Sorin Kihara; Stanley Bruckenstein

To cite this Article Fujinaga, Taitiro , Kihara, Sorin and Bruckenstein, Stanley(1977) 'Electrolytic Chromatography and Coulopotentiography - A Rapid Electrolysis at the Column Electrode used for the Preparation, Separation, Concentration, and Estimation of Trace and/or Unstable Substances', Critical Reviews in Analytical Chemistry, 6: 3, 223 — 254
To link to this Article: DOI: 10.1080/10408347708542693
URL: http://dx.doi.org/10.1080/10408347708542693

ELECTROLYTIC CHROMATOGRAPHY AND COULOPOTENTIOGRAPHY – A RAPID ELECTROLYSIS AT THE COLUMN ELECTRODE USED FOR THE PREPARATION, SEPARATION, CONCENTRATION, AND ESTIMATION OF TRACE AND/OR UNSTABLE SUBSTANCES

Authors: **Taitiro Fujinaga**
Department of Chemistry
Faculty of Science
Kyoto University
Kyoto, Japan

Sorin Kihara
Japan Atomic Energy Research Institute
Tokai-mura, Naka-gun, Ibaragi-ken
Japan

Referee: Stanley Bruckenstein
Department of Chemistry
State University of New York
Buffalo, New York

TABLE OF CONTENTS

I. INTRODUCTION

This article deals with a new analytical methodology based on rapid electrolysis on one hand and liquid phase chromatography on the other. From the standpoint of rapid electrolysis, many attempts in the instrumentation have been made. Eckfeldt[1] used a small cell (1.5 ml) with a working electrode of relatively large surface area to achieve a rapid electrolysis and determined iodide and dissolved oxygen in a flowing sample. In 1963, Fujinaga with other collaborators[2] investigated a rapid electrolysis at a series of column electrodes with silver grain as the electrode material. The electrode potentials of column electrodes were kept at different potentials. They termed the procedure "electrolytic chromatography" and quantitatively separated copper, lead, and cadmium by the method.

In the same year, Bard[3] used platinum gauze as the working electrode, agitated with nitrogen gas and ultrasonic wave, and achieved a quantitative electrolysis within 70 sec (λ = 0.1 sec^{-1}, see Section IV. A). Fujinaga et al.[4] developed a column electrode of continuous potential gradient and of programmed potential control against the reference electrode. As reported in their paper, they investigated precise experimental conditions for the consecutive determination of metals; conditions examined included species of electrode materials, grain size of the working electrode, species and flow rate of the carrier-supporting electrolyte solution, material of semipermeable membrane between working and auxiliary electrodes, composition of the counter electrodes, etc. The recommended conditions are discussed later in the text. Roe[5] suggested amalgamated nickel powder as an electrode material to be applied to electrochemical fractionation. Eckfeldt and Shaffer[6] determined dissolved oxygen using silver grains as the working electrode.

Blaedel and Strohl[7] used graphite grains as the material for a working electrode in the preparation of cerium (IV); in the differential reduction of Iron (III) and uranium (VI); and in the deposition of copper, lead, cadmium, and zinc. Then, they[8] discussed the relationship between the electrode potential and the retention time at the column electrode of amalgamated platinum grains in the deposition of thallium, lead, tin, and indium. Finlayson and Mowat[9] introduced tantalum gauze for the preparation of uranium (IV). Johansson[10] developed a rotating platinum gauze electrode, which reached the value, λ, of 0.18 sec^{-1} in the determination of silver and copper. Takata and Muto[11] determined gold, copper, and iron by flow coulometry at the platinum coil electrode. Okazaki[12] and Fujinaga et al.[13] analyzed the characteristics of the cell and the column electrode of glassy carbon grain; the λ value reached 1.0 sec^{-1}, and the quantitative electrolysis was performed within 7 sec. Recently, a few authors

discussed basic characteristics of the column electrolysis, such as current (coulomb)-potential curves[14] and relationships between the limiting current and the flow rate of the carrier solution.[15] In combination with other technical developments, the electrolytic chromatography has been utilized in various investigations, the details of which have been summarized[16,17] and are discussed further in the following sections.

From the chromatographic standpoint, many separation methods have been proposed based on a heterogeneous phase formation, such as adsorption, ion exchange, solvent extraction, etc. Recently, most of these methods, except precipitation and electrolysis, have been applied to the multistage separation technique, i.e., chromatography.

As is discussed later, electrolytic chromatography utilizes the principle of controlled potential electrolysis: it produces a separated and localized deposition of metals followed by stepwise dissolution. For the detection and determination of metals in the effluent, DC and AC amperometric, spectrophotometric, radiometric, and coulometric methods were employed as necessary. The use of radioactivity was extremely effective in the detection of trace amounts if the active isotope was available. The method of coulometric detection was the most successful in the sense that it is relatively sensitive, versatile to most of the metals examined, and convenient as it uses the same principle, i.e., electrolysis at the column electrode.

In the course of the study of flow coulometric detection, the method with controlled potential scanning, called coulopatentiography, gave more precise and selective quantitative data than conventional flow coulometry at constant potential. As the amount of electricity, i.e., coulomb, is recorded against the applied potential and the coulomb-potential curve appears similar to the current-potential curve in the conventional voltammetry, the authors[18] proposed the name of "coulopotentiography" for the method. One of the advantages of coulopotentiography over other voltammetric methods is that the absolute determination of amounts is possible without preparing a standard. Moreover, by combining anodic stripping, very high detection sensitivity with high specificity can be obtained; anodic stripping coulopotentiography detects metals of a concentration down to 10^{-9} mol/l.

In this review, some applications of analysis of metals, preparation of unstable substances, and elucidation of reaction mechanisms are presented together with instrumentation and theories of column electrolysis.

II. PRINCIPLE

The principle of electrolytic chromatography is schematically shown in Figure 1. Tube AB is the chromatographic column, in which an electrically conductive material is packed. DC voltage is applied to the conductive electrode material so that the inlet side will be positive and the potential gradient from C to D will be formed in the column. Therefore, if a carrier solution containing some electroreducible substances flows through the column from A to B, the substances may be locally deposited on the electrode according to their electromotive series: noble metals may be deposited close to C and less noble metals close to D. After the deposition is completed, the applied voltage is lowered while flowing the carrier solu-

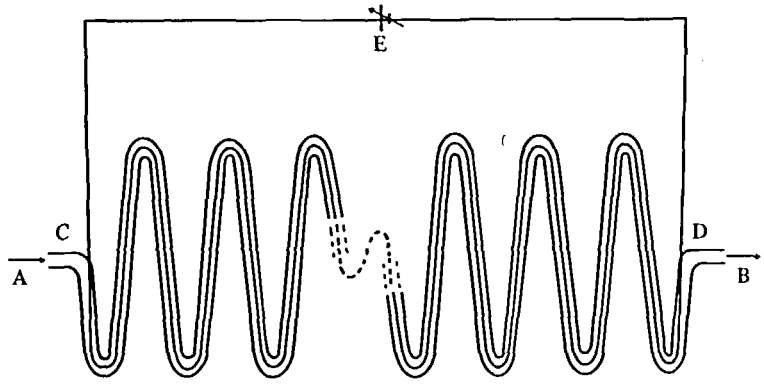

FIGURE 1. Principle of the electrolytic chromatograph.

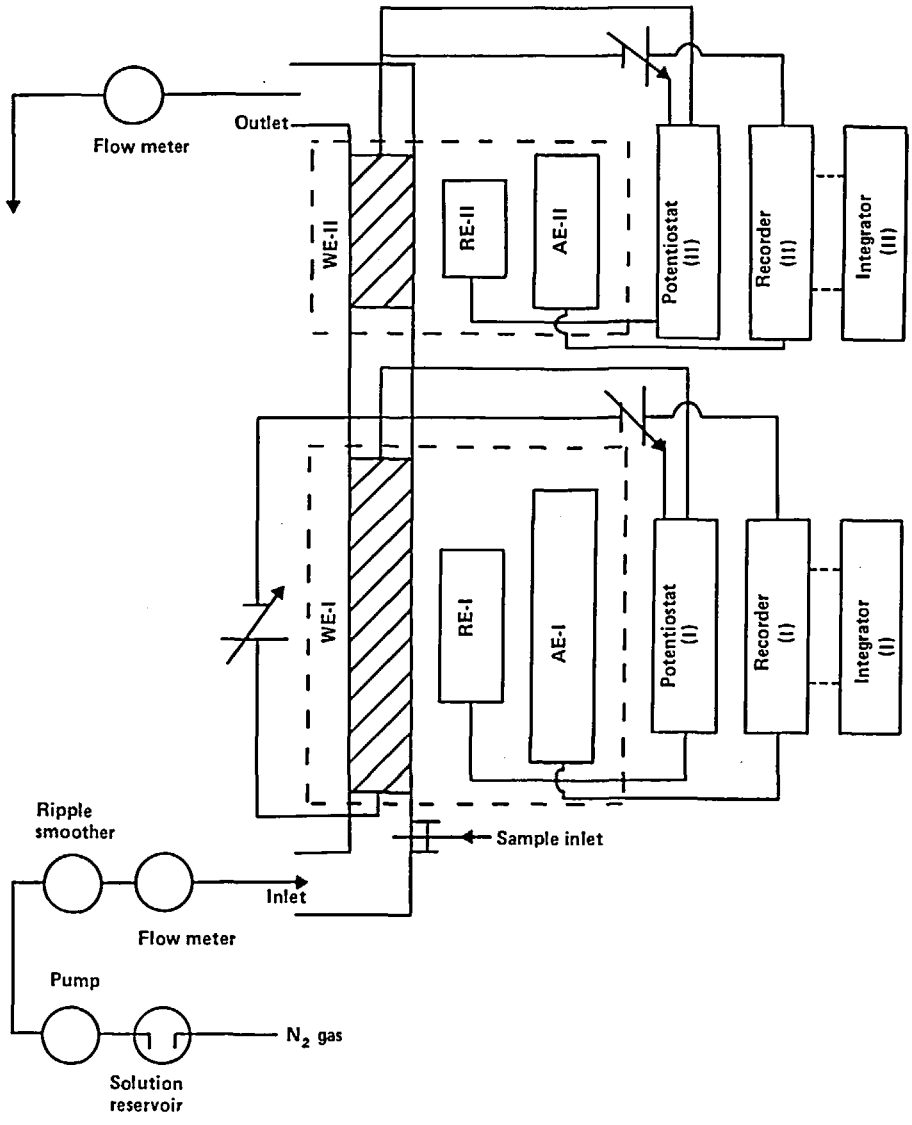

FIGURE 2. Schematic apparatus of electrolytic chromatograph with coulometric detector. (WE) Working electrode. (AE) Auxiliary electrode. (RE) Reference electrode. (E-I) Chromatographic column electrode. (E-II) Detector column electrode.

tion; the deposited metals may dissolve out successively. The metal coming out from outlet B may be determined by the flow coulometric method or by other possible detection methods.

The total set-up of practical electrolytic chromatography is shown in Figure 2. As seen from the figure, the carrier solution which contains the supporting electrolyte and which is deaerated, if necessary, flows continuously through the chromatographic and detector columns. The sample solution, usually less than 0.1 ml, is injected into the system ahead of the chromatographic column. As the potential of the chromatographic column is properly controlled, the metal ions in the sample are separated while flowing through the column and are conveyed into the detector cell one after another. The detector column, controlled at a proper potential, coulometrically measures the amount of each ion; the result is recorded as a current-time curve or a coulomb-time curve. Other methods of detection, e.g., radiometric or spectrophotometric methods, were also used; however, unless otherwise mentioned, coulometric detection is applied as shown in Figure 2.

III. INSTRUMENTATION

Potentiostats used for the control of electrode potential of the working electrode of both the detector cell and the chromatographic cell have the same characteristics, i.e., maximum electrolytic current: 250 mA, maximum terminal voltage: 15 V, maximum set voltage: 0 ± 2.00 V with the accuracy of ± 0.001 V and the response rate of 10^{-6} sec, input impedance: 10^{10} Ω, and set voltage switching velocity: 10^{-2} sec.

The block diagram of the potentiostat is shown in Figure 3. The main part consists of the operational amplifiers of all transisterized integrated circuits and programming mechanisms composed of an electric timer and many switches set to the proper signal voltages to be applied to the column electrode at a predetermined time.

Figure 4 shows three types of chromatographic and detecter cells. The working electrode of each cell was filled with 60 to 100 mesh glassy carbon grains (prepared by the Tokai Denkyoku (Electrode) Manufacturing Company) or with glassy carbon fibers 10 to 12 μm in diameter (made by Tokai Denkyoku (Electrode) Manufacturing Company or the Nippon Kayaku Company). Electroylsis was performed between the column electrode of the glassy carbon grains or glassy carbon fibers packed in a porous glass or porcelain tube. The counter electrode of silver wire or glassy carbon fiber was wound around the outside of the tube, which was inserted into an outer plastic tube containing an anolyte solution.

The current-time curve at the cell is recorded by a potentiometer recorder. The number of coulombs is calculated from the area under the current-time curve or is indicated directly by an integrator mounted ahead of the recorder (Photos 1 and 2).

IV. THEORY

Time Required for the Quantitative Electrolysis

Electrolysis is a heterogeneous reaction at a solid/liquid interface; it is, therefore, a relatively slow process. In conventional electrolytic analysis, it takes from 10 min to several hours to obtain a quantitative result.

In the presence of supporting electrolytes, the rate of mass transfer in the electrode process is mainly controlled by diffusion. Therefore, the rate of decrease in concentration of the metal ion in

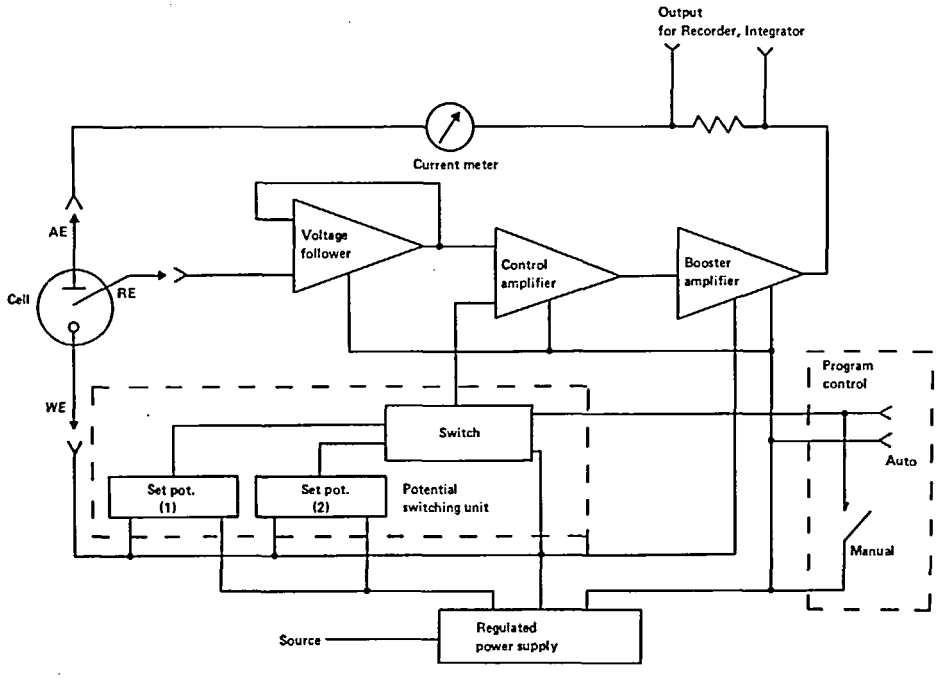

FIGURE 3. Block diagram of the potentiostat.

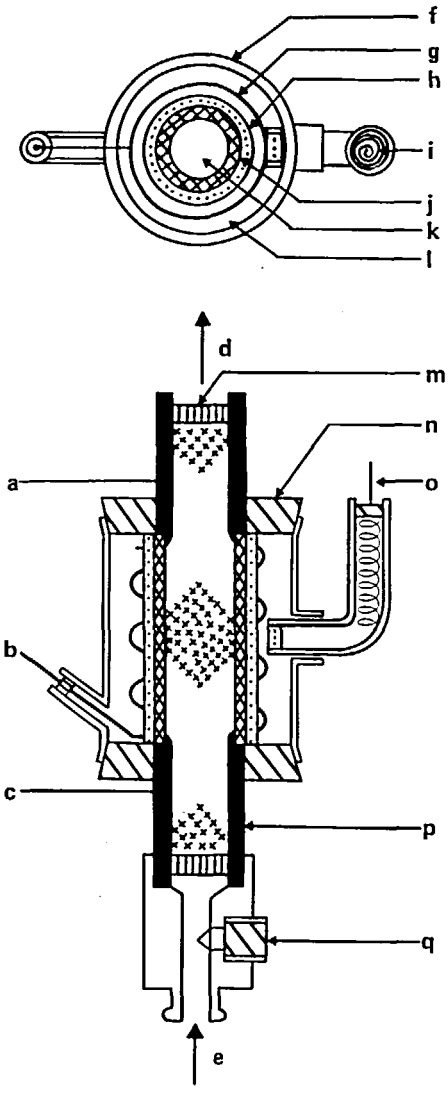

A.

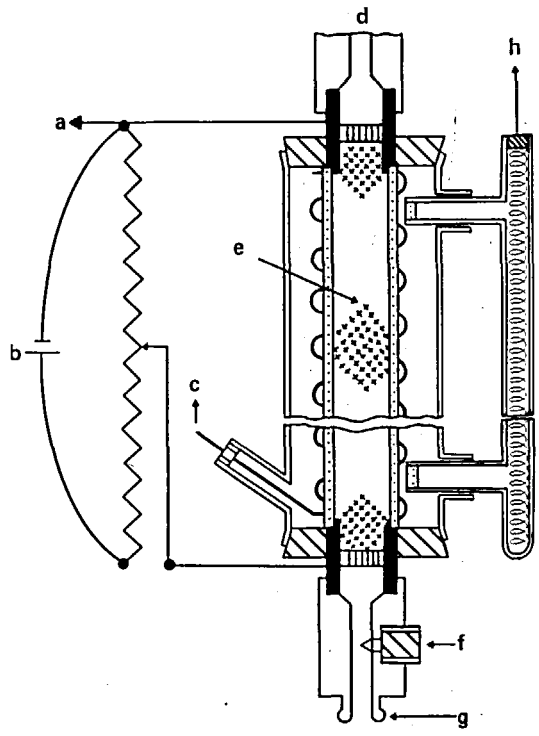

B.

FIGURE 4. Actual design of chromatographic and coulometric column electrodes. (A) Column electrode for coulometry: (a, c) lead for working electrode; (b, g) silver wire auxiliary electrode; (d) solution outlet; (e) solution inlet; (f) glass or plastic tube; (h) porous glass or porcelain tube; (i) silver spiral wire electrode; (j, p) porous carbon tube; (k) glassy carbon grains working electrode; (l) saturated KCl solution; (m) glass wool; (n) silicone rubber; (o) silver-silver chloride reference electrode, SSE. (B) Column electrode with gradient potential for electrolytic chromatography: (a) lead to potentiostat; (b) potentiometer; (c) silver wire auxiliary electrode; (d) solution outlet; (e) glassy carbon grains working electrode; (f) sample inlet; (g) solution inlet; (h) silver-silver chloride reference electrode, SSE. (C) Two-step column electrode for uniform potential electrolytic chromatography and elucidation of reaction mechanisms: (a) glassy carbon fibers working electrode; (b) glassy carbon fibers auxiliary electrode; (c) silver-silver chloride reference electrode, SSE; (4) porcelain cylinder; (d) saturated KCl solution; (e) sample inlet; (E-I) preparatory column electrode; (E-II) detector column electrode.

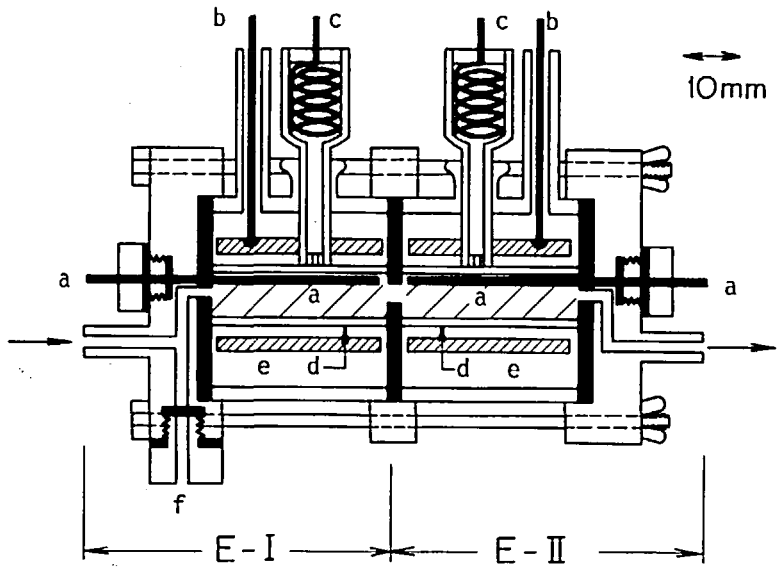

FIGURE 4C

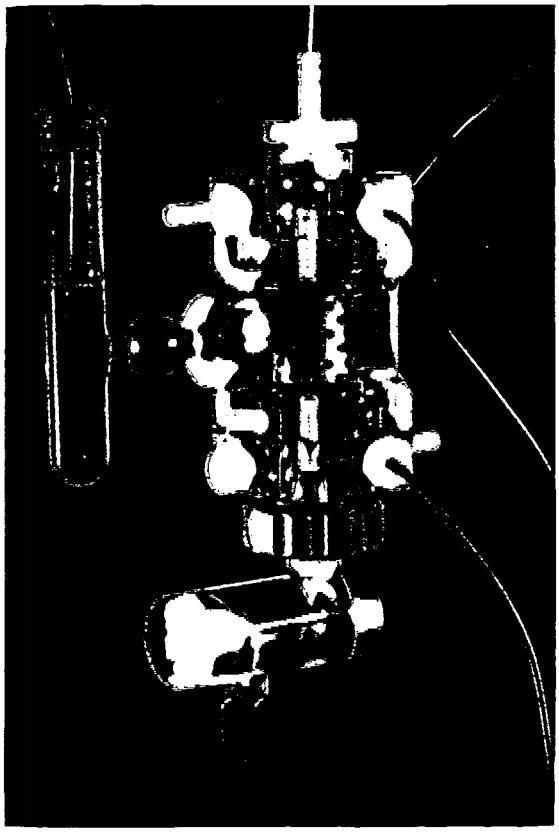

PHOTO 1. Standard type cell used for electrolytic chromatography and detection with reference electrode (left) and sample injection inlet (below). (Courtesy of Shibata Chemical Instrument Manufacturing Company, Ueno, Tokyo, Japan.)

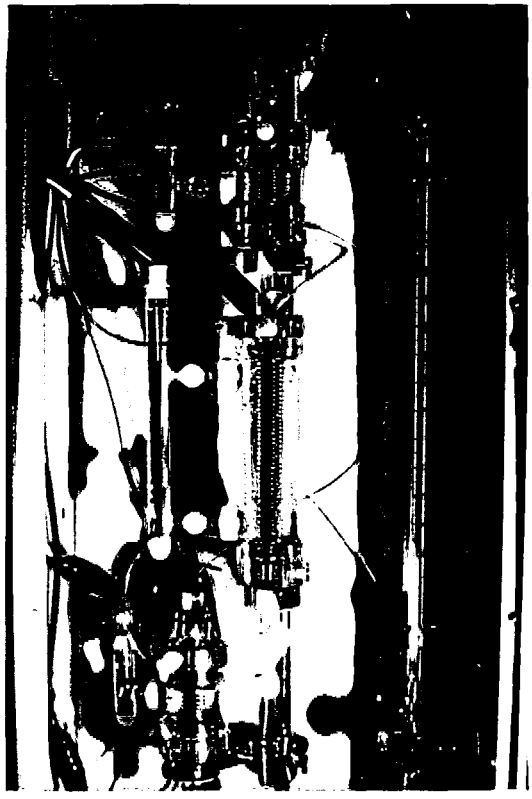

PHOTO 2. Detector cell (above), chromatographic cell (center), and pretreatment cell (below) with flow-rate meter.

solution or in current due to the electrolysis of the metal ion is proportional to the present concentration of the metal ion or the present current, respectively. Then,

$$-dc/dt = \lambda c \quad (1)$$

$$-di/dt = \lambda i \quad (2)$$

Here, λ is the proportional constant, called attenuation constant of the cell. Therefore, a current at time t is given by the following equation.

$$i = i_o \exp(-\lambda t) \quad (3)$$

Now if the time (t) is defined as the time when 99.9% of the metal ion is electrolyzed, i.e., when i/i_0 reaches 10^{-3}, then

$$t = 6.9/\lambda \quad (4)$$

In conventional electrolysis, more than 20 min is needed to obtain quantitative deposits; the attenuation constant (λ) never exceeds 0.005 sec.

Lingane[19] represented λ as a function of the diffusion coefficient (D $cm^2 \cdot sec^{-i}$), the surface area of the electrode (A cm^2), the thickness of the reaction layer (δ cm), and the volume of the electrolytic solution (V cm^3).

$$\lambda = DA/\delta V \quad (5)$$

According to Equation 5, more rapid electrolysis can be expected by increasing D and A and with decreasing δ and V. As described above, many efforts have been made to carry out electrolysis where the value of λ is large; however, λ has never reached a value over 0.1. The column cell described above and shown in Figure 4 has an extremely large surface area (A) relative to the cell volume (V). The value of λ reached 1.0 sec^{-1} with glassy carbon grains and 1.5 sec^{-1} with glassy carbon fibers as electrode materials. As can be seen from Figures 5 and 6, the electrolysis is completed within 7 sec with carbon grain electrodes and 5 sec with carbon fiber electrodes.

In practice, the current-time curve and the integrated current (coulomb)-time curve were recorded as shown in Figure 7. The curves are reproducible within the error of 0.1%, the main source of which seems to be introduced by sample injection with a syringe, i.e., the inaccuracy of the injection volume.

B. Chromatographic Consideration

As Blaedel[8] discussed, the distribution coefficient is so sharply dependent on the electrode potential that with a column electrode of uniform potential distribution, effective chromatographic separation is hardly expected.

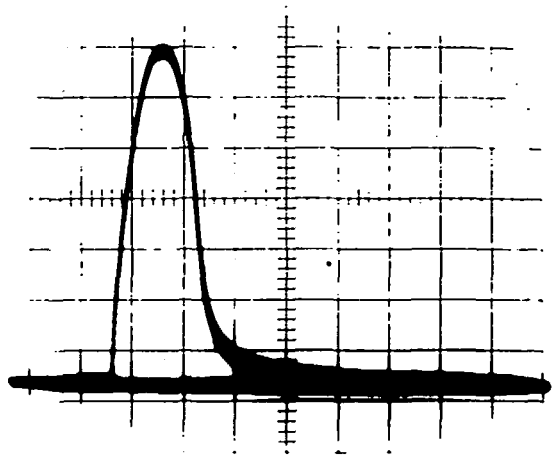

FIGURE 5. Oscillograph obtained in the electrolytic deposition of 5 μl of 1.0×10^{-2} *M* Pb^+ solution injected into the carrier stream. (Vertical axis) 0.4 mA/div. (Horizontal axis) 2 sec/div.

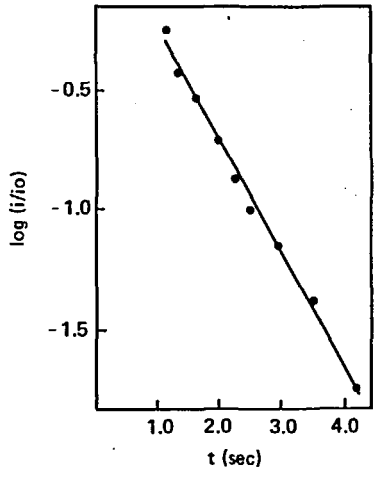

FIGURE 6. Analysis of current-time curve data taken from Figure 5.

When the following electrode reaction proceeds reversibly at the electrode surface:

$$M^{n+} + ne \rightleftarrows M \quad (6)$$

The Nernst equation holds as:

$$E = E^\circ + (RT/nF) \ln[M^{n+}]/[M] \quad (7)$$

Therefore, the distribution coefficient (K_D) is given by:

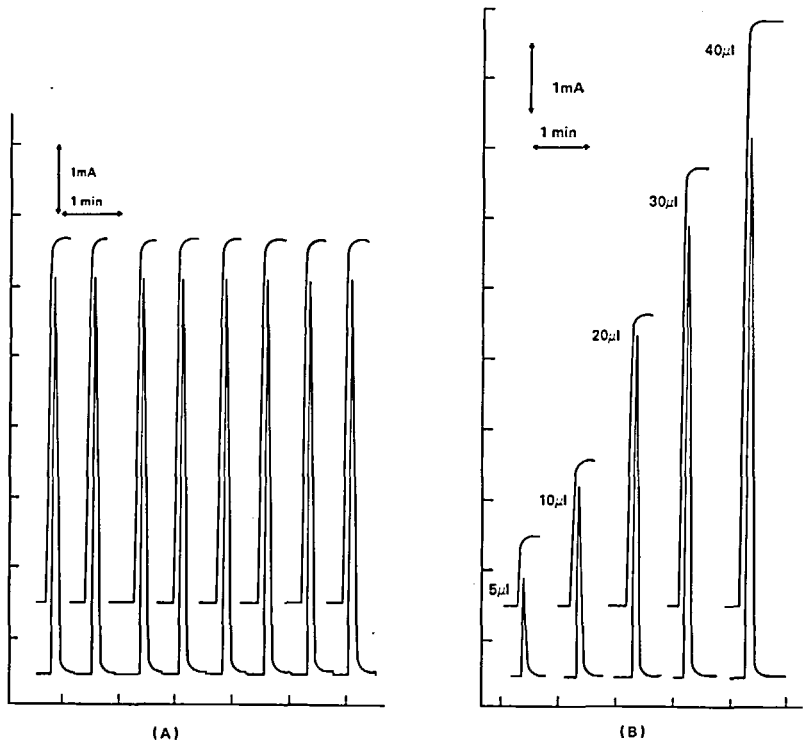

FIGURE 7. Coulometric curves of lead ions. Carrier solution: 0.1 *M* HCl. Flow rate: 3.5 ml/min. Electrode potential: −0.6 V vs. SSE. Sample: 1.00×10^{-2} *M* Pb^{2+}; (A) 25 μl, (B) 5, 10, 20, 30, and 40 μl.

$$K_D = [M]/[M^{n+}] = 10^{\frac{n(E^\circ - E)}{0.0591}} \text{ at } 25^\circ C \qquad (8)$$

Equation 8 shows that the distribution coefficient differs ten times with the change of 0.0591/nV. Accordingly, at the constant potential column electrode, metal ions, whose standard potential is more positive than the column potential, are deposited quantitatively and show large retention volumes. On the other hand, metal ions whose standard potential is more negative than the column potential pass together through the column at zero retention volume. This means that at the constant potential column all the metal ions are separated into two groups, a retained and an eluted. In order to improve the situation, the authors tried to use: (1) a series of column electrodes having stepwise electrode potential and (2) a long column electrode having a gradient electrode potential. In either case, the potentials were properly selected by the manual or programmed switching; thus, selective deposition and/or elution can be performed. Relevant details are presented below.

C. Nature of the Coulomb-potential Curve at the Column Electrode

The coulomb-potential curve was obtained by successively injecting samples and measuring the net quantity of electricity at a series of fixed potentials (E) of the column electrode.* The coulopotentiogram (Q-E curve) was quantitatively discussed by Kihara[14] on the basis of the work done by Levich[20] and Blaedel and Klatt.[21] Sioda[22,23] and Sioda and Kambara[15] examined the relation between the limiting current and the flow rate of carrier solution. Klatt and Blaedel[24] extended the study of a tubular electrode to the quasireversible and irreversible charge transfer systems.

In the case of the column electrode of which a working electrode is made from carbon fibers, the solution path in the electrode can be assumed to be an assembly of tubular electrodes of small radius. Therefore, comparing the conception of the current-potential curve at the tubular electrode to the current (coulomb)-potential curve at the column electrode, we can obtain the basic nature of column electrodes.

*A new method of automatic recording of the coulopotentiogram was developed recently[33] (see Section VII).

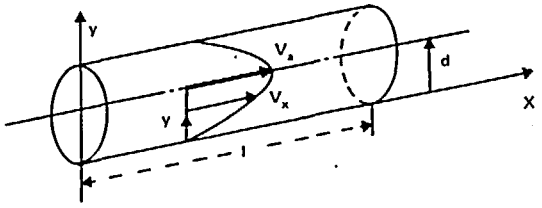

FIGURE 8. Mass transfer model at the tubular electrode.

When the reversible electrode reaction is between soluble oxidant Ox and soluble reductant Red, the reaction takes place in the following way at the tubular electrode.

$$Ox + ne \rightleftarrows Red \tag{9}$$

Linear velocity of solution V_x at the point (x,y) in Figure 8 is given by

$$V_x = V_a\left[1 - \frac{(d-y)^2}{d^2}\right] \tag{10}$$

where

V_a = the axial linear velocity;
x = distance parallel to the stream;
y = distance from the electrode surface;
d = the diameter of the tubular electrode.

When the stream is fast enough, $d \gg y$; then,

$$V_x = \frac{2V_a y}{d} \tag{11}$$

According to Levich, the mass transfer flux is given by:

$$V_x \frac{\partial C_i}{\partial x} = D_i \frac{\partial^2 C_i}{\partial y^2} \tag{12}$$

Therefore, soluble oxidant and reductant are transferred in accordance with the following equations:

$$\frac{2V_a y}{d}\frac{\partial C_{ox}}{\partial x} = D_{ox}\frac{\partial^2 C_{ox}}{\partial y^2} \tag{13}$$

$$\frac{2V_a y}{d}\frac{\partial C_{red}}{\partial x} = D_{red}\frac{\partial^2 C_{ox}}{\partial y^2} \tag{14}$$

At the point far enough from the electrode surface, the concentrations (C_{ox}, C_{red}) of depolarizers are equal to those (C^*_{ox}, C^*_{red}) in the solution. Next, at the electrode surface, the sum of the mass transfer of both depolarizers to and from the electrode is equal to zero, and the concentrations are defined by the Nernst equation. Accordingly, when $y = \infty$,

$$C_{ox} = C^*_{ox} \tag{15}$$

$$C_{red} = C^*_{red} \tag{16}$$

When y = 0,

$$D_{ox}\frac{\partial C_{ox}}{\partial y} + D_{red}\frac{\partial C_{red}}{\partial y} = 0 \tag{17}$$

$$\theta = \frac{C_{ox}}{C_{red}} = \exp\left[\frac{nF}{RT}(E - E_0)\right] \tag{18}$$

The decrease of Ox at the electrode surface due to the electrode reaction (Equation 9) is given by the flux of the substance Ox obtained from the solution of Equations 13 to 18.

$$\frac{dN_{ox}}{dt} = 2\pi d\int_0^X D_{ox}\left(\frac{\partial C_{ox}}{\partial y}\right)_{y=0} dx$$

$$= -KD_{ox}^{2/3} f^{1/3}\left(\frac{C^*_{ox} - \theta C^*_{red}}{1 + k\theta}\right) \tag{19}$$

where

k = $(D_{ox}/D_{red})^{2/3}$;
X = the effective length of the tube for substance Ox;
N_{ox} = the amount of Ox in moles;
K = a characteristic constant for the electrode.

Constant K involves an effective cross section of solution path term and a term for the effective surface area for the depolarizer. Here, as the radius of the solution path is sufficiently smaller than its length in the column electrode, it is assumed that the variation of bulk concentration of Ox may be proportional to the decrease of Ox at the electrode surface. When N_0 mol of total amount of Ox and Red in a u-liter volume of sample solution is introduced into the column electrode, Equation 19 can be rewritten as Equation 21 using:

$$\lambda = KD_{ox}^{2/3} f^{1/3} \tag{20}$$

$$\frac{dC^*_{ox}}{dt} = \frac{1}{u}\frac{dN_{ox}}{dt} = -\lambda\frac{C^*_{ox} - \theta\left(\frac{N_0}{u} - C^*_{ox}\right)}{1 + k\theta} \tag{21}$$

Then, the concentration of Ox at time t, $C^*_{ox,t}$, is given as the following equation by using the initial condition: $t = 0, N_{ox} = xN_0$,

$$C^*_{ox,t} = \frac{N_0}{u}\left[\frac{\theta}{1+\theta}\left\{1 - \exp\left(-\frac{1+\theta}{1+k\theta}\cdot\frac{\lambda t}{u}\right)\right\}+ x \exp\left(-\frac{1+\theta}{1+k\theta}\cdot\frac{\lambda t}{u}\right)\right] \quad (22)$$

where

x = the mole ratio of Ox in the sample solution.

From Equations 21 and 22, the current i_t at time t is given as:

$$i_t = -nF\frac{dN_{ox}}{dt} = \frac{\lambda nFN_0}{u}\cdot\frac{\theta(x-1)+x}{1+k\theta} \exp\left(-\frac{1+\theta}{1+k\theta}\cdot\frac{\lambda t}{u}\right) \quad (23)$$

Total electricity (Q_T) for the period 0 to T is

$$Q_T = \int_0^T i_t\,dt \quad (24)$$

$$= nFN_0\left(x - \frac{\theta}{1+\theta}\right)\left[1 - \exp\left(-\frac{1+\theta}{1+k\theta}\cdot\frac{\lambda T}{u}\right)\right]$$

As the current is controlled by diffusion, the limiting coulomb (Q_{dc}) at the cathodic process is given by:

$$\theta = 0 : Q_{dc} = nFN_0\left[1 - \exp\left(-\frac{\lambda T}{u}\right)\right] \quad (25)$$

and the limiting coulomb (Q_{da}) at the anodic process is given by:

$$\theta = \infty : Q_{da} = -nFN_0(1-x)\left[1 - \exp\left(-\frac{\lambda T}{ku}\right)\right] \quad (26)$$

From Equation 25, the electrolytic efficiency (ϵ) of the column electrode with diffusion controlled electrode reaction can be obtained as:

$$E = 1 - \exp\left(-\frac{\lambda T}{u}\right) \quad (27)$$

The time(T) in which substance Ox passes through the column electrode can be expressed by using the length of the column (L), the volume flow rate (f), and the effective cross-sectional area of solution path (S);

$$T = SL/f \quad (28)$$

Finally, the relation between E, f, and L is given by Equations 20, 27, and 28.

$$\log(1-\epsilon) = -K'f^{-2/3}D_{ox}^{2/3}SLu^{-1} \quad (29)$$

where

K' = constant.

From Equations 18, 24, 25, and 26, when k is nearly unity, the relation between coulomb and potential can be expressed approximately by the following equation:

$$E = E_0 - \frac{RT}{nF}\ln\left(\frac{D_{ox}}{D_{red}}\right)^{2/3} + \frac{RT}{nF}\ln\left(\frac{Q_{dc}-Q_T}{Q_T-Q_{da}}\right) \quad (30)$$

Equation 30 represents the coulopotentiographic curve (Q-E curve), and the half-coulomb potential ($E_{1/2}$) is a constant defined as:

$$E_{1/2} = E_0 - \frac{RT}{nF}\ln\left(\frac{D_{ox}}{D_{red}}\right)^{2/3} \quad (31)$$

The nature of the Q-E curve, therefore, resembles that of the polarographic i-E curve (Figure 9).

In the case of the totally irreversible process (Figure 10), the Q-E curve is represented by the following equation for the cathodic process[14]:

$$E = E_0 - \frac{RT}{\alpha nF}\left[\ln\frac{uf}{k_sASL} + \ln\left(\ln\frac{Q_{dc}}{Q_{dc}-Q_T}\right)\right] \quad (32)$$

where

α = the transfer coefficient;
A = the effective surface area of the electrode;
k_s = the standard rate constant.

V. ELECTROLYTIC CHROMATOGRAPHY AT THE UNIFORM POTENTIAL ELECTRODE[25]

In simple electrolytic chromatography, two column cells of the same dimension, shown in Figure 4C, were used. The first cell acted as the chromatographic cell to differentiate mixed components, to concentrate trace components, to remove some interfering components, or to prepare a uniform oxidation state of a component in question; the second cell acted as the detector

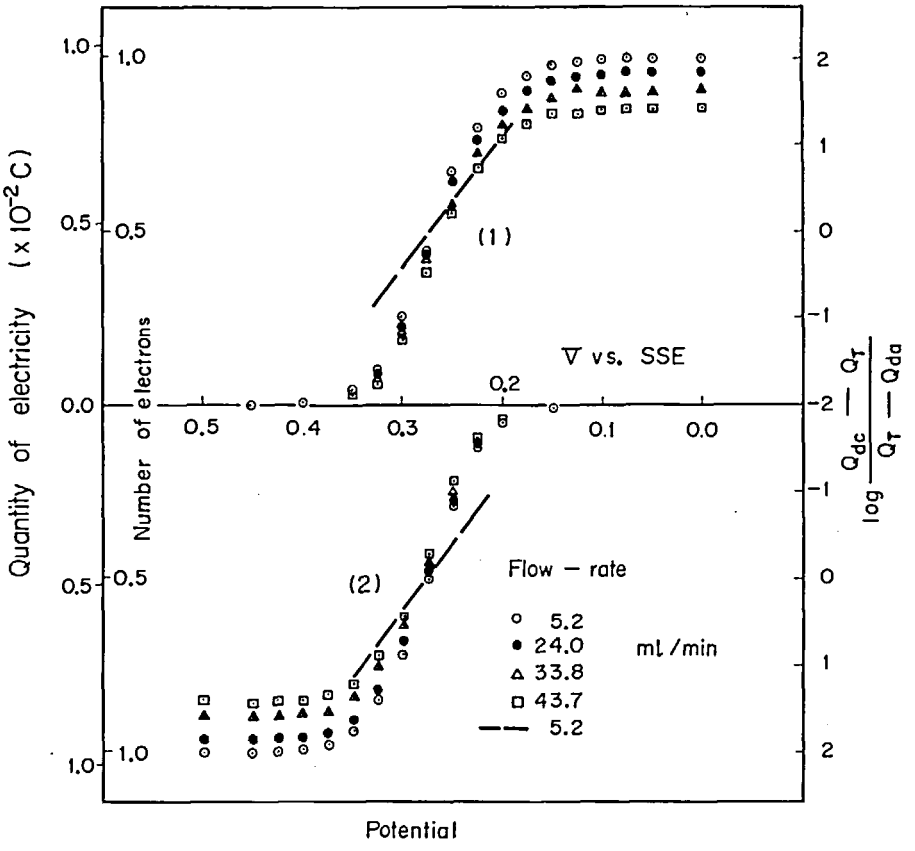

FIGURE 9. Typical coulopotentiogram for the reversible electrode reaction. Sample: 10^{-2} *M* $[Fe(CN)_6]^{4-}$ or $[Fe(CN)_6]^{3-}$, 10 μl (1.0×10^{-7} mol). Carrier solution: 1 *M* KCl solution. Column length: 2 cm. Working electrode: glassy carbon fibers. (----) Logarithmic analysis.

cell. This two-step combination was applied to the basic investigation of the column properties, to the analysis of various substances, and to the elucidation of the electrode reaction mechanism. Some of the experimental results are presented here.

A. Fundamental Investigations on the Column Electrode

Various kinds of experiments were carried out with lead and copper ions in the stream of 0.5 *M* perchloric acid solution. The mercurous sulfate electrode with 1*M* H_2SO_4 solution (MSE) was used as the reference electrode. The carrier solution of 0.5 *M* $HClO_4$ was kept in a one-liter reservoir and was supplied to the cell after deaeration by bubbling nitrogen gas into the reservoir. The flow rate was controlled by changing the height of the reservoir or by changing the pressure of nitrogen on it, if necessary. The working electrode (the glassy carbon grains) was pretreated in the carrier solution by applying +1.5 V for 5 min and then −1.5 V for 5 min. The procedure was repeated five times before use.

Deaerated carrier solution is allowed to flow through both cells (E-I and E-II). Potential of −1.10 V vs. MSE is applied to both the cells using two independent potentiostats (P-I and P-II); 1.0 to 100 μl of a sample solution is injected with a microsyringe. The deposition current flows in the first cell (E-I) circuit because both cupric and lead ions are reduced to the metallic state at the potential. Keeping the potential of E-II at −1.10 V, the potential of E-I is raised to −0.50 V. Lead in E-I is dissolved out, conveyed into the second cell (E-II), and reduced to a metallic state again when the deposition current flows through the cell circuit of E-II.

In a series of fundamental deposition-dissolution studies, it was demonstrated that the number of coulombs required in the metal deposition in E-I at −1.10 V was equal to that discharged in the dissolution in E-I at −0.50 V and also to

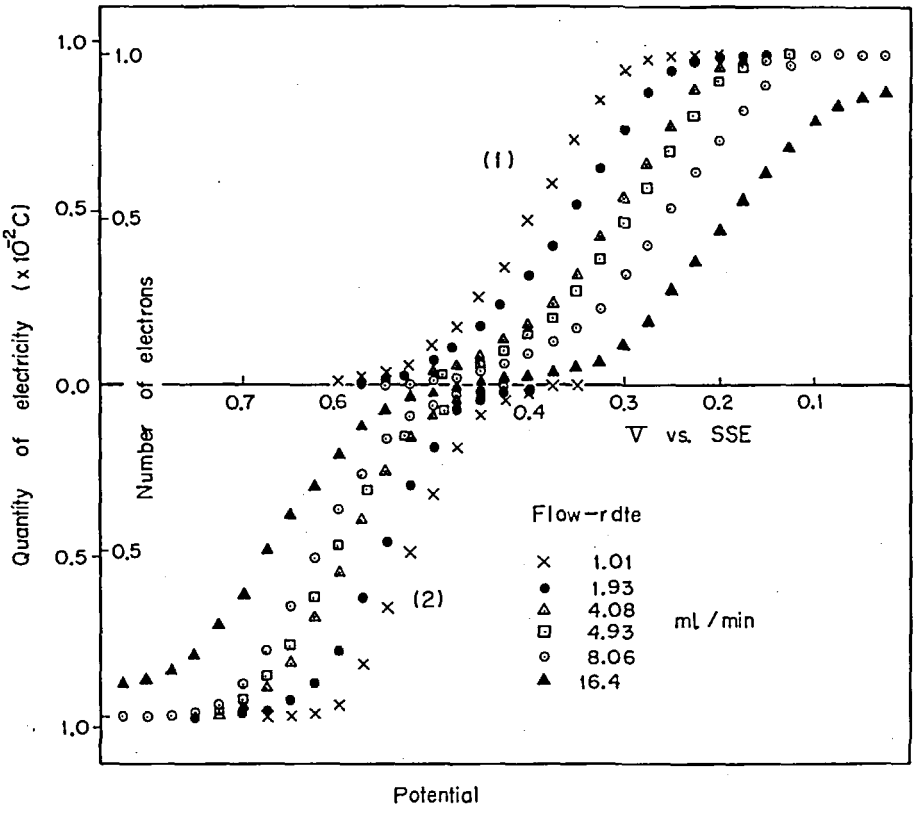

FIGURE 10. Typical coulopotentiogram for the totally irreversible electrode reaction. Sample: 10^{-2} *M* Fe^{2+} or Fe^{3+}, 10 μl (1.0×10^{-7} mol). Carrier solution: 1 *M* H_2SO_4 solution. Column length: 2 cm. Working electrode: glassy carbon fibers.

that required in the redeposition in E-II at -1.10 V. The amounts of electricity required and exhausted are in good agreement with those calculated by Faraday's electrochemical equivalency. Similar quantitative results were obtained in the deposition of copper ions at -1.10 V and in the dissolution at +0.20 V.

The most interesting phenomena were observed when the above experiments were carried out with a mixture of both lead and copper ions. As can be seen from the deposition and dissolution curves, when both lead and copper ions are injected one after another into E-I, both of the deposited ions dissolve out quantitatively at -0.50 and +0.20 V, respectively, irrespective of the order of injection, i.e., even when copper is introduced after lead, the lead is dissolved out quantitatively at -0.50 V (Figure 11). From the standpoint of analytical methodology, this phenomenon is extremely favorable, although the reason has not been made clear: the exchange dissolution of lead by copper and the redeposition of lead onto a farther part of

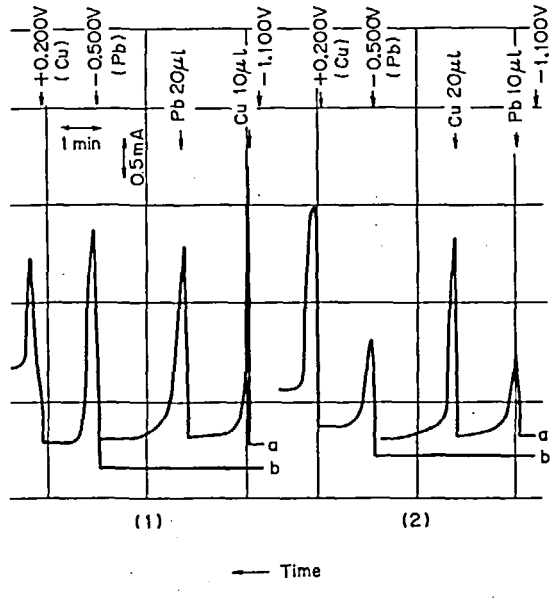

FIGURE 11. Effect of the order of electrodeposition on the separation of copper and lead. (a) Current at E-I. (b) Current at E-II.

the column would probably be taking place in the deposition step, and the localized deposits of both metals may dissolve out independently.

B. Successive Determination of Traces of Metals

In a carrier stream of 0.5 *M* perchloric acid, cadmium, lead, and copper ions were deposited onto glassy carbon fiber electrodes of E-I kept at -0.40 V vs. MSE and were eluted successively by raising potential: first at -1.00 V to dissolve cadmium, second at -0.50 V to dissolve lead, and finally at +0.20 V to dissolve copper. The determinations were made coulometrically at the detector cell E-2 whose potential was kept at -1.40 V vs. MSE.

In a solution of 0.5 *M* perchloric acid, lead and tin ions were reduced at the potentials close together, but the separation was possible by the careful selection of an elution potential at -0.925 V vs. MSE, where tin alone was eluted quantitatively.

Instead of injecting a small amount of sample solution into the carrier stream, extremely dilute solutions (i.e., 10 μl of $2.00 \times 10^{-8} M$ cadmium, lead, or copper solutions in 0.5 *M* perchloric acid) were passed through E-I at -1.40 V to concentrate them on the column; then, they were eluted at -1.00, -0.50, and +0.20 V, respectively. Averages of $1.92 \times 10^{-8} M$ for cadmium, $1.96 \times 10^{-8} M$ for lead, and $2.03 \times 10^{-8} M$ for copper were obtained. In conclusion, it was demonstrated that:

1. The successive determination of metals is possible by the proper control of the potential of the chromatographic column electrode in combination with the flow coulometric detection at the column electrode.
2. Even with a difference of 20 mV in the deposition potentials, the two metals can be quantitatively separated when the electrode processes are reversible (rapid).
3. By the use of preconcentration with the chromatographic cell, concentrations of metals down to $10^{-8} M$ can be determined by the present method.

C. Rapid Determination of Traces of Oxalate Ions[26]

Oxalic acid may be conveniently used for the removal of contaminants from the reactor because it dissolves most fission products, including uranium, as oxalate complexes and decomposes itself by radiation. Therefore, it becomes necessary to determine very dilute oxalate ions in strong radioactive solutions.

Coulomb-potential curves of various ions in 0.5 *M* sulfuric acid are shown in Figure 12. In the figure, it is shown that at +1.20 V vs. the saturated silver chloride electrode (SSE), chromate and ceric ions are reduced to Cr(III) and Ce(III) and ferrous and uranium ions are oxidized to Fe(III) and U(VI), respectively. On the other hand, at the potential of +1.60 V, none of these ions, i.e., Cr(III), Ce(III), Fe(III), and U(VI), is electrolyzed, but the oxalate ions are quantitatively oxidized. In conclusion, the following procedure is recommended for the determination: supporting electrolyte solution of 0.5 *M* sulfuric acid is flowed through the first cell, E-I, at +1.20 V vs. SSE and then the second cell, E-II, at +1.60 V. The 5- to 10-μl sample solution of 10^{-5} to 10^{-1} *M* oxalate ion is injected before the E-I cell, and the oxidation current of oxalate ions in the E-II cell is recorded. In the procedure, the E-I cell removes most of interfering substances except hydrogen peroxide. The oxalate ion is oxidized in the E-II cell according to the following mechanism:

$$C_2H_2O_4 \rightarrow 2CO_2 + 2H^+ + 2e^-$$

The time required for the determination is approximately 20 sec. 10^{-5} to 10^{-3} *M* oxalate ion can be determined within an error of 4% and above 10^{-3} *M* within 2%. Other carboxylic acids such as citric, formic, glycolic, and tartaric acid are not oxidized at +1.60 V. The interference from hydrogen peroxide can be eliminated by the addition of vanadyl ion (Figure 13).

Using the proposed method, the decomposition of oxalate ions by light was studied: with decreasing concentration of oxalate, the effect of radiation becomes more pronounced. In the presence of metal ions which have multiple oxidation states in aqueous solution, the oxalate ion decomposes more rapidly.

In conclusion, for the determination of oxalate, electrolytic chromatography is advantageous with respect to the small sample size, speed, high precision, and possibility of remote controlled analysis. The method is applicable in many cases.

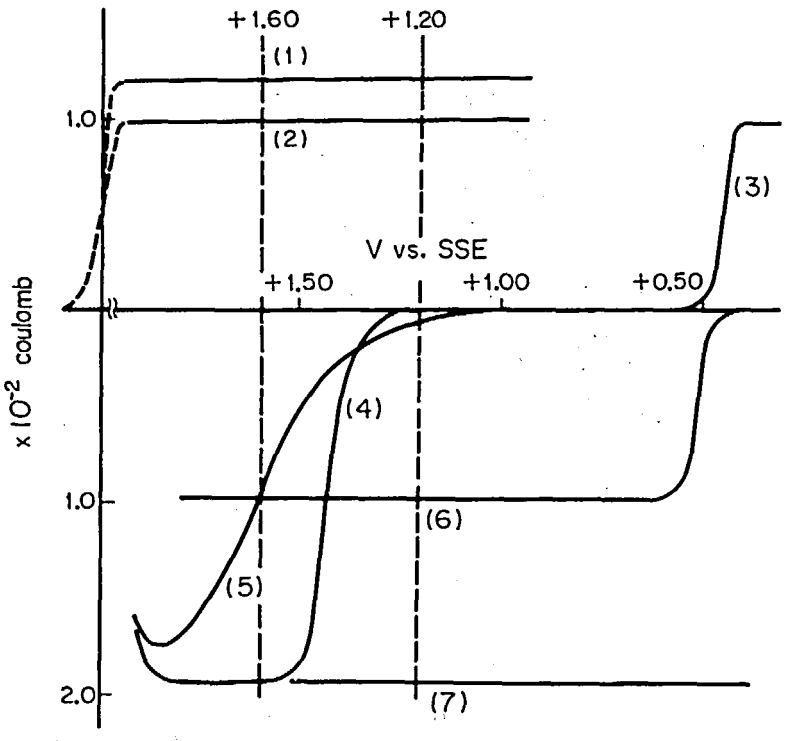

FIGURE 12. Coulomb-potential curves of various ions. (1) Cr(VI) + 3e→Cr(III). (2) Ce(IV) + e→Ce(III). (3) Fe(III) + e→Fe(II). (4) $C_2O_4^{2-} \rightarrow 2CO_2 + 2e$. (5) $H_2O_2 \rightarrow O_2 + 2H^+ + 2e$. (6) Fe(II)→Fe(III) +e. (7) U(IV)→U(VI) + 2e. Sample: 10 μl of $4.0 \times 10^{-3} M$ for Cr(VI) and of 1.0×10^{-2} for others. Flow rate: 10 ml/min.

D. Smoothing of Oxidation States and State Analysis[27]

For the purpose of preparing a sample solution of desirable oxidation states, a uniform potential column electrode has been extensively used in the authors' laboratories. The two-step flow coulometric system (Figure 4C) was effectively used in the study. The first cell, E-I, acts as a pretreatment apparatus to remove interfering elements in some cases and in other cases as a smoothing apparatus to make the oxidation state of the sample uniform before it enters into the detector column, E-II.

The proposed system was used to prepare an iron solution of uniform oxidation states and to determine the ratio of ferric to ferrous ions in an aqueous iron solution. In 0.5 *M* sulfuric acid solution, ferric ions are reduced completely at +0.5 V vs. SSE and ferrous ions are oxidized completely at +0.65 V vs. SSE. With the two column electrodes, the potential of E-I is controlled at +0.10 V and that of E-II at +0.65 V. Ten microliters of the iron solution, a mixture of 0.0106 *M* ferrous and 0.0094 *M* ferric ions, is injected into the column electrode. Figure 14 shows current-potential curves. The reduction begins 3 sec after sample injection at E-I (+0.10 V, curve 1), and after 6 sec the oxidation occurs at E-II (+0.65 V, curve 2). The arrow shows the time of sample injection. The oxidation curve of the sample at E-I with +0.65 V was obtained separately and added in Figure 14 (curve 3). The sum of the integrated values of curves 1 and 3 is equal to that of curve 2. Consequently, it is evident that the analysis of oxidation states in solution is possible from curves 1 and 2 by using the two-step coulometric system.

E. Elucidation of the Reaction Mechanism at the Glassy Carbon Electrode[14,28]

The two-step flow coulometric system is effective to elucidate the electrode reaction mechanism, particularly when the reaction products are unstable or oxidizable in air. A sample solution as small as 10 μl could be analyzed, and the unstable product with a half-life of 10^{-2} to 30 sec could be measured.

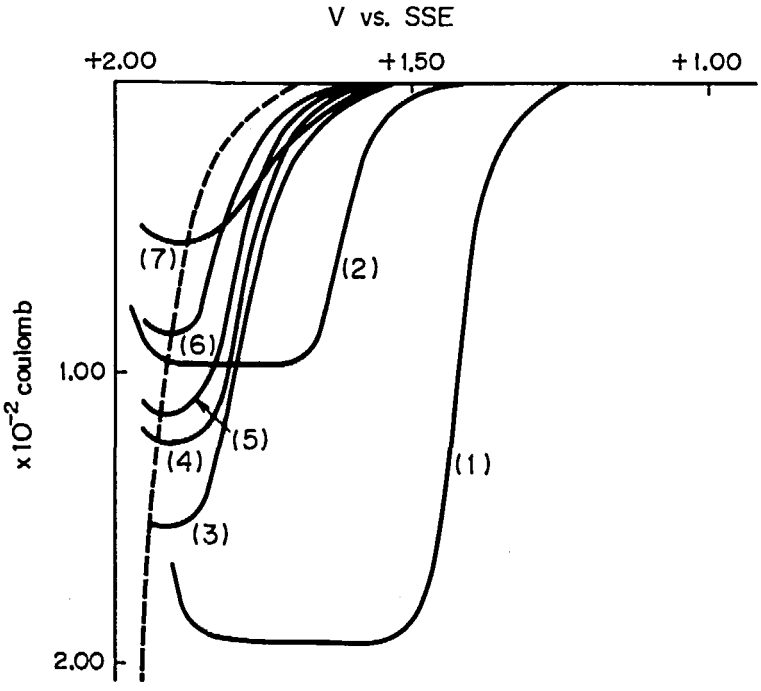

FIGURE 13. Coulomb-potential curves of various organic acids in 0.5 *M* H_2SO_4. (1) 10^{-2} *M* oxalic acid. (2) 10^{-2} *M* glyoxalic acid. (3) 10^{-1} *M* tartaric acid. (4) 10^{-1} *M* citric acid. (5) 10^{-1} *M* glycolic acid. (6) 10^{-1} *M* formic acid. (7) 10^{-2} *M* glyoxal. Succinic and acetic acid are not oxidized at potentials more negative than +1.9 V vs. SSE. Sample size: 10 μl. Flow rate: 10 ml/min.

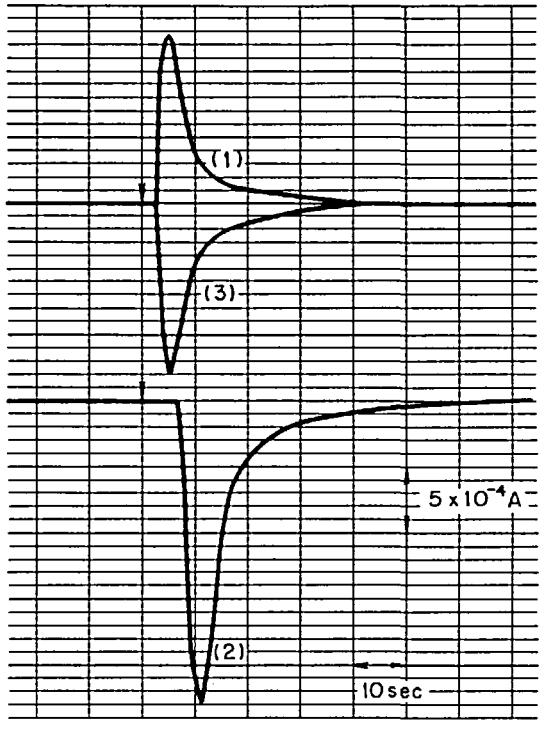

FIGURE 14. Current-time curves recorded with 10 μl of 1.06 × 10^{-2} *M* Fe(III) and 0.94 × 10^{-2} *M* Fe(II). Carrier solution: 0.5*M* H_2SO_4. Flow rate: 5 ml/min.

As a preliminary test, the electrolytic reduction of cupric ions was investigated: various kinds of coulomb-potential curves (Q-E curves) were obtained (Figure 15). These curves obtained by two-step flow coulometry are the same shape and give the same information as those obtained by rotating ring-disk voltammetry.

1. The quantity of electricity (Q_1) is measured at a definite potential (E_1) with a definite amount (10^{-7} mol; 10^{-2}*M*, 10μl) of cupric ion using E-I. The measurements of Q_1 are made at various potentials (E_1), and a Q_1-E_1 curve similar to the polarographic current-potential curve is obtained. The Q_1-E_1 curve shows two waves. Both correspond to one electron reduction; therefore, the first wave is the reduction to the cuprous state and the second wave, to the metal (curve 1).

2. The quantity of electricity (Q_2) was measured at the coulometric detector (E-II), at a constant potential (+0.50 V vs. SSE). The measurement of Q_2 was made at various potentials (E_1), and the coulomb-potential (Q_2 (+0.50 V)-E_1) curve was plotted, which is shown as curve 2. This curve clearly demonstrates that the cupric

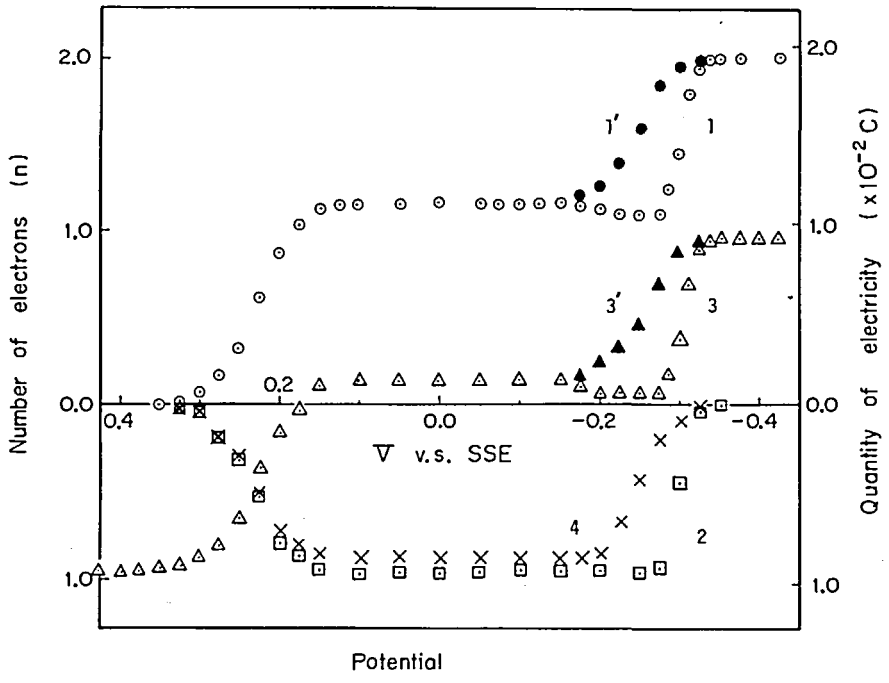

FIGURE 15. Coulomb-potential curves of copper in 0.1 *M* HCl-0.9 *M* KCl. Sample: 10^{-2} *M* Cu^{2+}, 10 μl (1.0×10^{-7} mol). Flow rate: 5.02 ml/min. Column length: 2 cm. Working electrode: glassy carbon fibers. Potential control (V vs. SSE): Curve 1, 1′ – E_1 = +0.50, E_2 variable; Curve 2, 2′ – E_1 variable, E_2 = +0.50; Curve 3, 3′ – E_1 = 0.00, E_2 variable; Curve 4 – E_1 = −0.50→variable, E_2 = +0.50. Curves 1′ and 3′ were obtained with copper-plated glassy carbon fiber working electrode.

ions are reduced at E-I with the potential ranging from +0.3 to −0.3 V to form cuprous ions, which are then oxidized to a cupric state at E-II, showing the oxidation current of curve 2. At a potential more positive than +0.3 V, cupric ions are not reduced; at a potential more negative than −0.3 V, all cupric ions are further reduced to the metallic state. Therefore, in both regions no current due to cuprous ions flows at E-II.

3. The quantity of electricity (Q_2) was measured at a definite potential (E_2) by using E-II. The potential (E_1) was kept constant at 0.0 V vs. SSE. The measurements of Q_2 were made at various potentials (E_2), and the Q_2-E_2 curve was plotted and shown as curve 3.

In order to elucidate the reaction mechanism of uranyl ions in chloride media, a similar investigation was carried out with a series of carrier solutions of varying acidity. Some of the results are shown in Figures 16 and 17.

Curve 1 in Figure 16 is the Q_1-E_1 curve of the reduction of uranyl ions (1.0×10^{-7} mol UO_2^{2+} in 0.1 *M* HCl and 0.9 *M* KCl). Curve 2 is the Q_2-E_2 curve of the reduction and oxidation of the mixture of UO_2^{2+} and small amounts of U(IV) prepared at E-I with E_1 = − 0.6 V. Curve 3 is the Q_2-E_2 curve of the oxidation of U(III) prepared at E-I with E_1 = −1.15 V. As can be seen from these curves, redox reactions of the UO_2^{2+}/UO_2^{+} couple proceed fairly reversibly, and U(IV) is oxidized to UO_2^{2+} at a potential more positive than the oxidation of UO_2^{+}. At the potential range from −0.05 to +0.1 V, the oxidation currents of UO_2^{+} and U(III) ions are detectable, but that of U(IV) is not. The reduction products at E-I with various potentials are detected at E-II with E_2 = +0.05 V. The results, Q_2(+0.05 V)-E_1 curve, are shown as curve 4 in Figure 17. This curve is obtained by plotting Q_2 at E-II with E_2 = +0.05 V against various potentials E_1 at E-I. The minimal quantity of electricity at the potential near −1.0 V shows

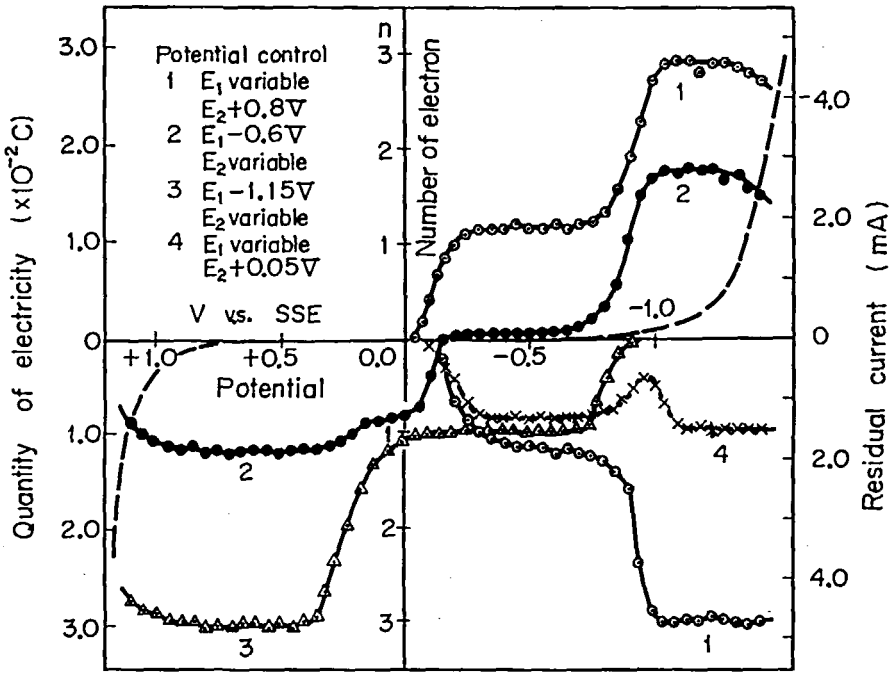

FIGURE 16. Coulomb-potential curves of uranium in chloride solution. Sample: $10^{-2}M$ UO_2^{2+}, 10 μl (1.0×10^{-7} mol). Carrier solution: 0.1 *M* HCl-1.9 *M* KCl. Flow rate: 1 ml/min. Column length: 4 cm. (---) Residual current.

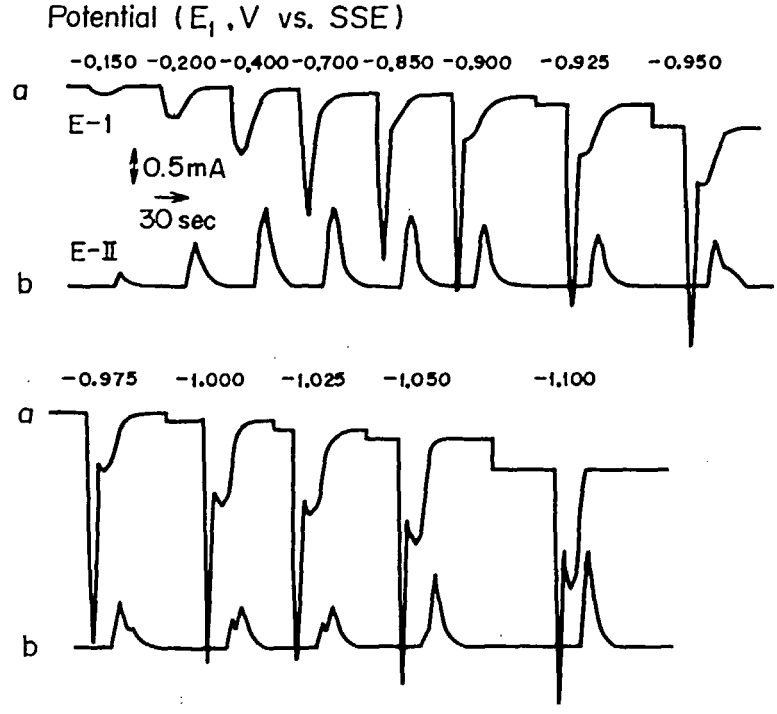

FIGURE 17. Current-time curves for reduction and oxidation of uranium in 0.1*M* HCl-1.9 *M* KCl. Sample: $10^{-2}M$ UO_2^{2+}, 10 μl (1.00×10^{-7} mol). Flow rate: 1 ml/min. E_2 = +0.05 V vs. SSE (constant).

that the reduction of UO_2^+ to U(III) proceeds via U(IV) step. The current-time curves corresponding to curves 1 and 4 in Figure 16 are shown as curves a and b in Figure 17. In the potential range from -0.15 to -0.7 V, the peak of E-I in curve a shows the reduction of UO_2^{2+} and the peak of E-II in curve b shows the reoxidation of UO_2^+. At potentials more negative than -0.85 V, another new peak appears in the curve of E-I. This new peak indicates the further reduction of UO_2^+. The peak of E-II begins to decrease at $E_1 = -0.85$ V; at potentials more negative than -0.925 V, a new peak begins to appear and the first peak is displaced by the new peak at $E_1 = -1.10$ V. The decrease of the first peak indicates that U(IV) is generated, and the appearance of the second peak indicates that U(III) is prepared at E-I.

In low acidity chloride media (2.0 *M* KCl, pH 3.5, unbuffered), the reduction and oxidation of the UO_2^{2+}/UO_2^+ system show fairly reversible properties, but the reduction of UO_2^+ occurs at the potential more positive than that at higher acidity (pH 2), as shown in Figure 18. The one-electron reduction product of UO_2^+ at E-I is deposited on the electrode surface and consequently is not detected at E-II, as shown by curve 1'. The Q-E curves (broken lines) for the reduction of UO_2^+ are irregular and not reproducible and have a gentle slope probably due to the hydrolysis of UO_2^+ or U(IV).

The comparison of the coulometric results at the two-step column electrode with the polarographic observations at the dropping mercury electrode is very interesting; it will, however, be discussed elsewhere.

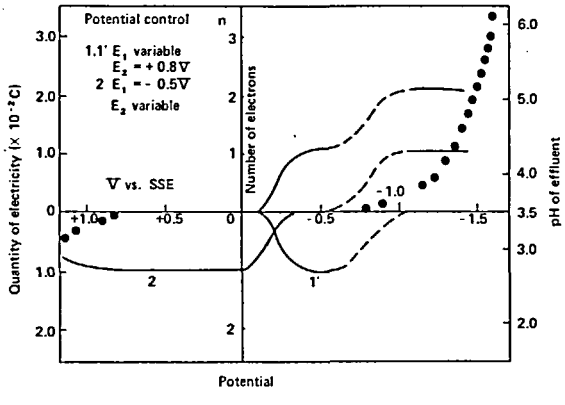

FIGURE 18. Coulomb-potential curves of uranium in 1.0 *M* KCl (ph 3.5, unbuffered). Sample: $10^{-2}M$ UO_2^{2+}, 10 μl (1.00×10^{-7} mol). Flow rate: 1 ml/min. Column length: 4 cm.

F. Determination of Plutonium in the Presence of Other Metal Ions[27]

The aim of this study is to analyze plutonium in the presence of other metals in a shielded glove box as a protection from its strong activity and poison. Plutonium is well known to have many oxidation states, such as $Pu(VI)O_2^{2+}$, $Pu(V)O_2^+$, Pu(IV), and Pu(III), in aqueous solution. Moreover, oxidation states of plutonium are unstable due to the disproportionation or air oxidation reactions. It is difficult to prepare a solution of uniform ionic state by simple chemical procedures.

In the present study, two-step column electrolysis was applied. The first cell was used to remove interfering elements and at the same time to smooth the oxidation state of plutonium; the second cell was used to coulometrically measure the amount of plutonium.

Figure 19 shows coulomb-potential curves of plutonium and some other elements in 0.5 *M* H_2SO_4. It was experimentally confirmed that plutonium exists as a mixture of Pu(III) and Pu(IV) in 0.5 *M* H_2SO_4.[29] From the Figure, it becomes clear that Pu(III) and Fe(II) are quantitatively oxidized and Cr(VI) and Ce(IV) are quantitatively reduced at +0.75 V, but other elements are not affected. When the sample enters the second column, quantitative reduction of Pu(IV) and Fe(III) proceeds at +0.10 V, whereas other elements are not electrolyzed. That is to say, the element from which a coulomb-potential curve arises between the potentials of E-I and E-II interferes with the determination of plutonium, but other elements do not. To eliminate the interference of iron, potentials of E-I and E-II must be chosen more severely, e.g., $E_1 = +0.75$ V, $E_2 = +0.45$ V as shown in Table 1.

As for the results, the following procedure is recommended for the semiautomatic analysis of plutonium. A 0.5 *M* H_2SO_4 solution as carrier is continuously allowed to flow through the two column cells and the potential of the first cell is controlled at +0.75 V and that of the second cell at +0.45 V using two independent potentiostats. The sample solution is introduced into the carrier

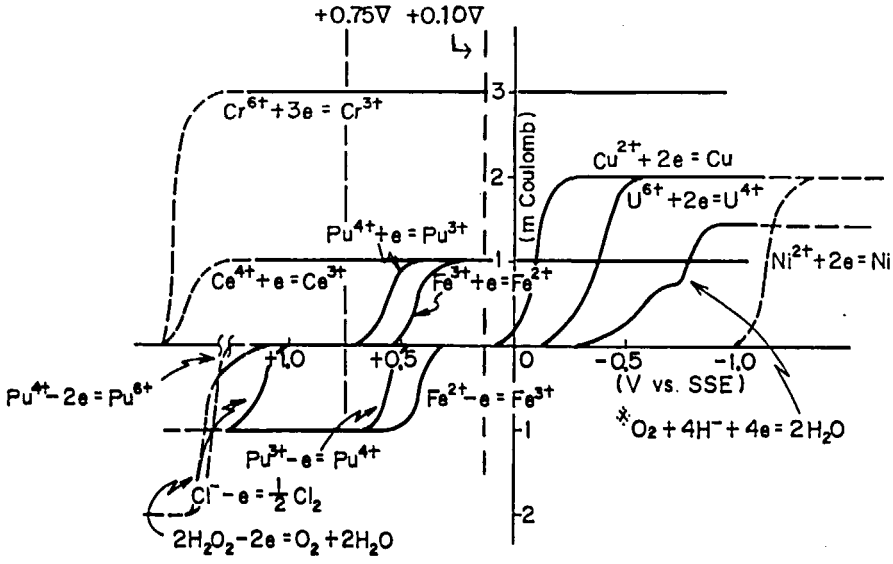

FIGURE 19. Coulomb-potential curves of plutonium and other metal ions. Sample: 10^{-8} mol, 10 µl of air-saturated 0.5 *M* H_2SO_4. Carrier solution: 0.5 *M* H_2SO_4. (Broken lines) Oxidation or reduction of medium took place prior to those of samples.

TABLE 1

Determination of Plutonium in the Presence of Iron

E_2 V vs. SSE	Electricity consumed: Calculated (C)	Electricity consumed: Found (C)
+0.500	$2.017\ 10^{-3}$	$1.27\ 10^{-3}$
		1.39
		2.41
+0.475	$2.017\ 10^{-3}$	$1.89\ 10^{-3}$
		1.81
		1.97
+0.450	$2.017\ 10^{-3}$	$2.20\ 10^{-3}$
		2.21
		2.23
+0.425	$2.017\ 10^{-3}$	$2.24\ 10^{-3}$
		2.31
		2.30

Note: Sample – 2.09×10^{-8} mol Pu, 2.00×10^{-8} mol Fe. Carrier solution – 0.5 *M* H_2SO_4. Flow rate – 5 ml/min, E_1 = +0.75 V vs. SSE.

stream. As the sample contains both Pu(III) and Pu(IV), the current recorder of the first column measures the quantity of Pu(III) due to the reaction Pu(III) $-e \rightarrow$ Pu(IV). The current recorder of the second column measures the quantity of Pu(IV) based on the reaction Pu(IV) $+e \rightarrow$ Pu(III); hence it represents the sum of Pu(III) and Pu(IV) in the sample.

If the sample contains ferrous iron or other reducible substances, the first recorder will measure them in addition to Pu(III). However, the second recorder measures only Pu(IV) and not other ions because they are hardly reduced at +0.45 V; Ce(IV) and Cr(VI) are reduced at the first column (E_1 = +0.75 V), and Fe(III), Ce(III), Cr(II), Cu(II), Ni(II), U(VI), and Cl^- are neither reduced nor oxidized at the second column (E_2 = −0.45 V). Hence, few ions interfere with the determination of plutonium. Various amounts of plutonium (mixture of III and IV) were analyzed, and the results are summarized in Table 2. The effect of various ions is shown in Table 3.

In conclusion, the proposed analytical method is accurate within ± 3% with 0.05 ml of 4×10^{-3} *M* Pu(III and IV) solution and is sensitive down to 0.02 ml of 2×10^{-5} *M* Pu. The determination is automatically performed except for the introduction of samples.

The determination of the ratio of plutonium to uranium is often important because the mixed oxides or carbides are used as nuclear fuels. A coulometric procedure similar to that described above was developed as follows. A 100-mg sample of the mixed oxide was dissolved in 5 ml of 10 *M*

TABLE 2

Determination of Plutonium

Pu taken	$\times 10^{-8}$ mol taken	Coulomb calculated	Coulomb found	Pu found (%)
1.03 mg/ml	21.5	2.08×10^{-2}	2.04×10^{-2}	98.1
50 μl			2.07	99.5
			2.06	99.0
			2.01	96.7
			2.04	98.1
515 μg/ml	10.8	1.04×10^{-2}	1.05×10^{-2}	100.9
50 μl			1.03	99.0
			1.03	99.0
			1.04	99.6
			1.05	100.9
51.5 μg/ml	1.08	1.04×10^{-3}	1.07×10^{-3}	102.8
50 μl			1.04	99.6
			1.05	100.9
			1.03	98.9
			1.05	100.9
10.3 μg/ml	0.22	2.08×10^{-4}	2.20×10^{-4}	105.9
50 μl			2.07	99.6
			2.02	97.1
			2.15	103.5
			2.05	98.5
5.0 μg/ml	0.042	4.02×10^{-5}	3.97×10^{-5}	98.7
20 μl			3.94	98.0
			4.07	101.1
			3.93	97.8
			3.92	97.5

Note: Carrier solution – 0.5 *M* H_2SO_4. Flow rate – 5 ml/min. E_1 = +0.35 V, E_2 = +0.75 V vs. SSE.

TABLE 3

Determination of Plutonium in the Presence of Various Ions

Pu taken ($\times 10^{-8}$ mol)	Pu found ($\times 10^{-8}$ mol)	%
4.18	4.12	101.2
	4.07	99.9
	4.19	102.7
	Other ions present	
	Ce: 6.42 (10^{-8} mol)	
	Cr: 16.0	
	Cu: 4.01	
	Ni: 8.00	
	U: 3.98	
	Cl: 8.00	

Note: Carrier solution – 0.5 *M* H_2SO_4. Flow rate – 5 ml/min. E_1 = +0.75 V, E_2 = +0.10 V.

HNO_3 and three drops of 1 *M* HF. The solution was nearly evaporated to dryness. The addition of HNO_3 and HF and the evaporation were repeated three times, followed by dissolution with 25 ml of 0.5 *M* H_2SO_4. Ten microliters of the aliquot was taken as the sample and injected into the carrier stream of deaerated 0.5 *M* H_2SO_4. For the determination of plutonium, the potential, E_1, of the first column was kept at +0.10 V vs. SSE, and the quantity of electricity, Q_2, consumed at the second column was measured at the potential, E_2, of +0.75 V. For the determination of uranium, E_1 was kept at +0.10 V and Q_2 was measured at -0.60 V. Therefore, the electrode reactions of $Pu^{3+} - e \rightarrow Pu^{4+}$ and $U^{6+} + 2e \rightarrow U^{4+}$ were used, respectively, for the determinations. The results of the determination by the proposed procedure are summarized in Table 4.

VI. ELECTROLYTIC CHROMATOGRAPHY AT THE GRADIENT POTENTIAL ELECTRODE[30]

A. Separation of Cadmium, Lead, and Copper

In the separation and determination of lead and copper, the chromatographic cell having the gradient potential column electrode shown in Figure 4B was used; this method could be considered liquid phase chromatography with the column of continuously changing partition coefficient. After thorough preliminary experiments with the coulomb-potential curves, the following conditions were found adequate for the determination.

A carrier solution of 0.5 *M* hydrochloric acid, deaerated by bubbling nitrogen gas, was passed through the column at the rate of 1.0 ml/min; the rate was controlled by a constant velocity pump. Then, -0.70 V against SSE was applied to the outlet part of the chromatographic cathode using a potentiostat, and a voltage drop of 0.30 V was applied along the column, resulting in the potential of the inlet part of the cathode being maintained at -0.40 V vs. SSE.

One to 100 μl of the sample solutions of 1.0×10^{-2} *M* lead and copper was introduced using a microsyringe, as is customary in gas chromatography. The cupric ions in the solution were first deposited at the inlet of the column, but the lead ions passed through it and were deposited close to the outlet. After several minutes the cathode potential of the outlet was raised to -0.40 V, resulting in an increase of the potential of the inlet to -0.10 V. By this procedure, lead was dissolved and conveyed into the coulometric detector cell, in which the cathode potential was set at -0.7 V vs. SSE, and copper was moved and redeposited at the outlet. After completion of the dissolution of lead, which could be seen on the coulometric recorder, again the cathode potentials were changed to $E_1 = E_2 = +0.40$ V. By this procedure, copper was transferred to the coulometric cell and the current was recorded (Figure 20).

Determinations were made with the solutions of lead and cupric ions in various ratios; the size of the sample solutions was 1 to 100 μl. The results obtained were satisfactory, with an accuracy of ±3% with 10-μl samples and ±5% with 1-μl samples.

B. Radiometric Determination of ThB, ThC, and ThC''

Electrolytic chromatography is especially suitable for rapid separation and can be operated under remote control, so that its application to the

TABLE 4

Determination of Plutonium in Plutonium-uranium Mixed Oxide Samples

Pu/Pu + U taken[a] (%)	Pu found (mg)	U found (mg)	Pu/Pu + U found (%)
25.0	21.83	65.53	24.97
	30.44	90.68	25.13
	22.13	66.15	25.06
30.0	33.25	82.20	28.80
	32.80	84.04	28.07
	32.76	80.01	29.02
33.0	24.27	49.83	32.75
	23.00	47.00	32.89

[a]These are the standard samples prepared at the Japan Atomic Research Institute.

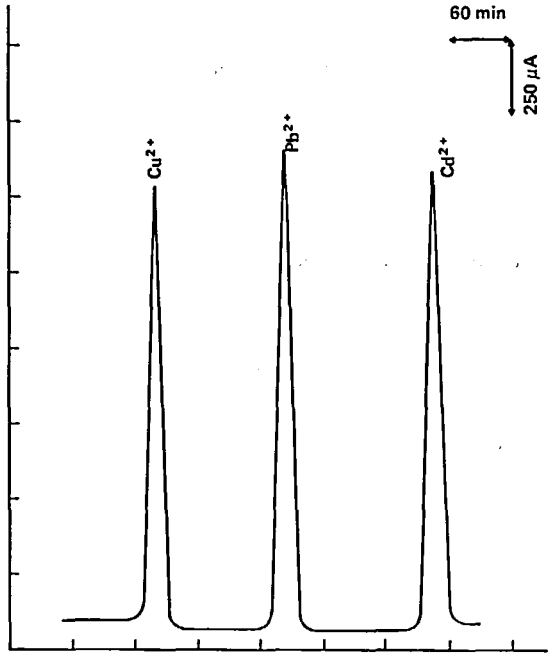

FIGURE 20. Successive determination of Cd^{2+}, Pb^{2+}, and Cu^{2+} with the potential gradient electrode. Sample: 1×10^{-7} mol.

separation of unstable radioactive nuclides is promising. This section deals with the quantitative aspects of the separation of ThB, ThC, and ThC″ as tracers of lead, bismuth, and thallium, respectively.

1. Reagent and Apparatus

A carrier-free solution of a mixture of ThB, ThC, and ThC″ in radioactive decay equilibrium was prepared from "radiothorium" from the Radiochemical Centre, Amersham according to the usual method. A single-channel pulse-height analyzer equipped with a 1.5 X 2 in. NaI well-typed crystal was used for the radioactivity measurements.

2. Experimental

The potential of the chromatograph column electrode was controlled so as to distribute between E_1 = -0.40 V vs. SSE at the inlet and E_2 = -0.70 V at the outlet. A deaerated solution of 0.5 *M* hydrochloric acid was passed through the system at 1 ml/min. From the injection inlet, 0.20 ml of the sample solution (containing ThB, ThC, and ThC″ with or without 1×10^{-2} *M* Pb^{2+} or Bi^{3+} as carrier) was introduced using a microsyringe.

By this procedure, ThC and bismuth ions were deposited at the inlet, ThB and lead ions at the outlet, and ThC″ came out immediately without deposition on the electrode at the potential. The solution coming out was divided into fractions of 1 ml each, always using a fraction collector after the sample introduction.

After 10 min the electrode potentials were changed to E_1 = 0.00 V and E_2 = -0.40 V. Then, ThB with lead ions was eluted out. Finally, the electrode potentials were adjusted to $E_1 = E_2$ = 0.00 V. Then, ThC with bismuth was dissolved and transported to the fraction collector.

It can be seen from the decay scheme of radiothorium shown in Figure 21 that ThB (half-life $t_{1/2}$ = 10.6 hr), ThC ($t_{1/2}$ = 60.5 min), and ThC″ ($t_{1/2}$ = 3.1 min) are the measurable nuclides when existing in equilibrium. Figure 22 shows the chromatograms of radioactivities obtained with the fractions collected by the procedure described. Decay curves for the three peaks are presented in Figure 23. As can be seen from the figures, the activities of the first chromatographic peak were eluted out with a very short retention time and showed a half-life of 3.3 min which agreed well

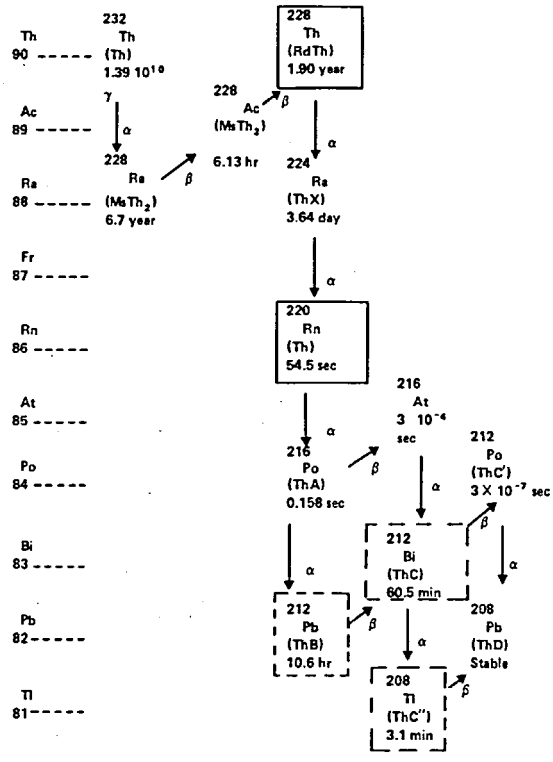

FIGURE 21. Decay scheme of Th series.

with that of ThC″. The activities of the second peak were eluted out when E_2 was changed to -0.40 V, and the half-life was measured to be 10.6 hr which is the same as the accepted value for ThB. The activities of the third peak resulted when E_2 became 0.00 V and a half-life of 60 min was obtained, in good agreement with the accepted value of 60.5 min with regard to ThC. The total recovery of the activities injected was 101.4% which indicates that the quantitative elution is possible with the glassy carbon grain electrode.

Figure 24 shows the elution curves of a carrier-free mixture of ThB, ThC, and ThC″ under the same experimental conditions; the concentrations of ThB, ThC, and ThC″ are approximately 10^{-11}, 10^{-12}, and 10^{-13} *M*, respectively. The results are summarized in Table 5. ThB and ThC in the sample were quantitatively deposited even from the extremely dilute solution and were eluted out anodically without leaving any detected activity due to absorption. When the sample solution was passed through the column in an open circuit, all of the radioactive compounds came out of the column, as shown in Table 5.

For the quantitative deposition of lead and

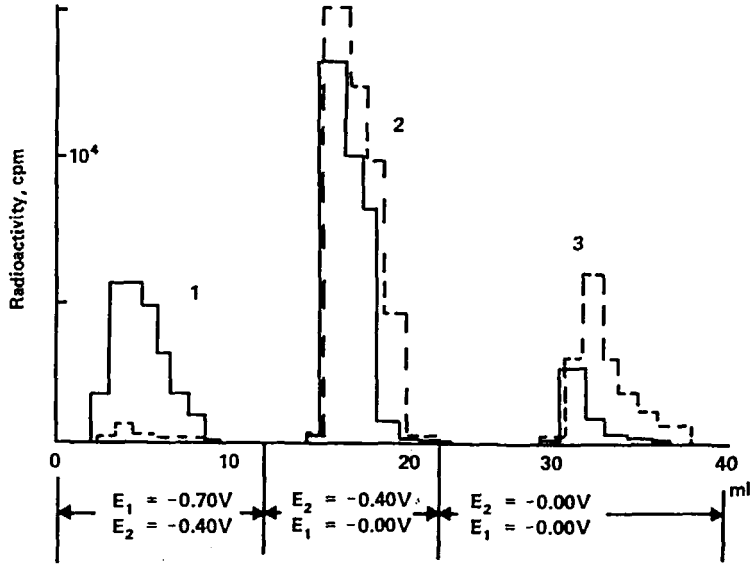

FIGURE 22. Elution chromatogram of radioactivities in the presence of their stable isotopes. Sample: 20-μl solution containing 2.0×10^{-7} mol Pb^{2+} (ThB), Bi^{3+}, and ThC″. Carrier solution: 0.5 *M* HCl. Flow rate: 1.0 ml/min. (Straight line) Histogram not corrected for decay. (Dotted line) Histogram corrected for decay. (1) ThC″ ($t_{1/2}$ = 3.1 min). (2) ThB ($t_{1/2}$ = 10.6 hr). (3) ThC ($t_{1/2}$ = 60.5 min).

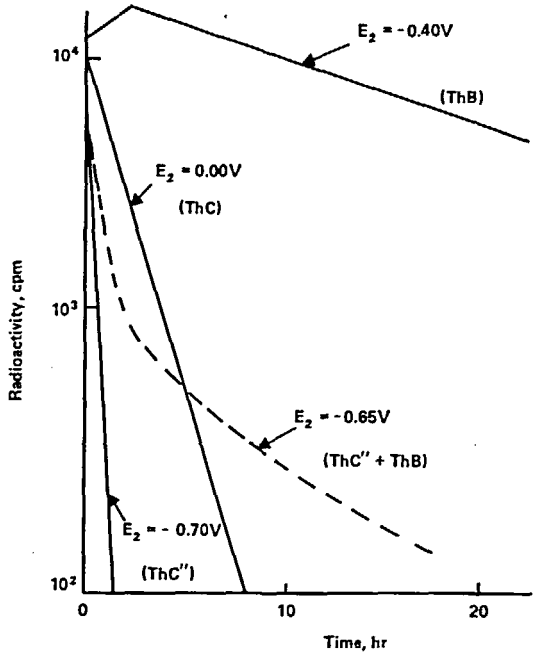

FIGURE 23. Decay curves of separated components.

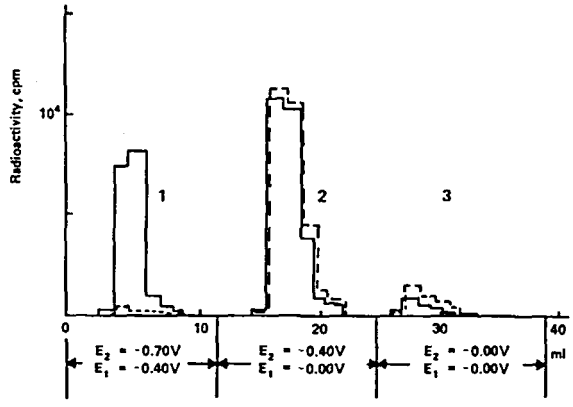

FIGURE 24. Elution chromatogram of carrier-free radioactivities. Sample: 20-μl solution containing about 10^{-16} mol ThB, 10^{-17} mol ThC, and 10^{-18} mol ThC″. Other conditions same as Figure 22. (1) ThC″ ($t_{1/2}$ = 3.1 min). (2) ThB ($t_{1/2}$ = 10.6 hr). (3) ThC ($t_{1/2}$ = 60.5 min).

ThB, the potential was more negative than -0.70 V. When the potential was maintained at -0.65 V, about 5% of the lead ions was eluted without being deposited. The electrode potential of -0.70 V was also sufficient for the quantitative deposition of carrier-free ThB.

The fact that the 10^{-11} *M* Pb^{2+} (ThB) solution was quantitatively electrolyzed at the same potential as the 10^{-2} *M* Pb^{2+} solution cannot be explained by the Nernst equation; under potential deposition is responsible, but further investigation must be carried out to solve this problem. ThC″, which is a daughter of ThC and is an isotope of thallium, was eluted out and isolated

TABLE 5

Recoveries of Radioactivities

Exp. no.	Radioactivities taken (cpm)	Radioactivities found (cpm) ThC″	ThB	ThC	Total	Recovery (%)
1[a]	19,532	(No applied voltage)			19,183	98.3
2[b]	18,400				18,097	98.0
3[a]	46,750	17,763	26,690	2,221	46,675	99.9
4[b]	58,336	19,075	34,896	5,238	59,209	101.4

Note: All activities are corrected for decay.

[a]Carrier free: ThC″ = 10^{-16} mol, ThB = 10^{-14} mol, ThC = 10^{-15} mol.
[b]With carrier: ThC″ = 10^{-16} mol, ThB + Pb^{2+} = 2 × 10^{-7} mol, ThC + Bi^{3+} = 2 × 10^{-7} mol.

from other species without being deposited; it was the first time that ThC″ was successfully isolated, because its half-life is too short (3.1 min) for the effective isolation by the conventional electrolytic method.

VII. COULOPOTENTIOGRAPHY AT THE COLUMN ELECTRODE

In the course of the study of electrolytic chromatography, a kind of new voltammetric method at the column electrode was developed in these laboratories.[33] The new method is carried out with scanning the potential and deals with a flowing solution which contains the supporting electrolyte and intended depolarizer.

At the column electrode, the electrolysis proceeds very rapidly if the electrode potential is selected properly to obtain the limiting current. Then, the number of coulombs (Q) required is proportional to the electrochemical equivalent (W) and hence to the concentration (C) of the depolarizer, volume (V) of the solution, and number (n) of electrons involved in the reaction

$$Q = 96500W = 96500nCV \quad (33)$$

Therefore, the instantaneous electrolytic current is proportional to the concentration as shown by the following equation:

$$I = \frac{dQ}{dt} = 96500nC\frac{dV}{dt} = 96500nCf \quad (34)$$

where

f = the flow rate (l/sec) of the solution.

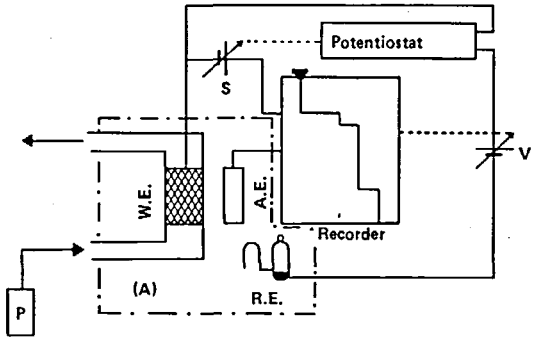

FIGURE 25. Block diagram of the coulopotentiograph. (A) Column electrode. (W.E.) Working electrode. (A.E.) Auxiliary electrode. (R.E.) Reference electrode. (V) Voltage scanner. (S) Electrolysis source. (P) Volumetric pump.

Accordingly, if the electrolytic current is recorded against the applied voltage according to the proper conditions mentioned below, the curve appears in a shape similar to that of the polarogram, and the limiting current gives the concentration of the depolarizer in the solution. Moreover, the estimation of concentration can be made by Equation 34 without preparing the standard. Figure 25 shows the schematic diagram of the new method termed "coulopotentiography." Part A is the column electrode. The carrier solution, in which both the depolarizer and the supporting electrolyte are dissolved, is made to flow through the column electrode by a volumetric pump (P). The scanning potential is applied to the working electrode (W.E.). The potential is scanned by a voltage scanner (V) and is controlled against the

reference electrode (R.E.) by a potentiostat. The instrumentation is identical to that of the polarography of the three-electrode system.

A. Nature of the Coulopotentiogram[32]

On the basis of the discussion for the mass transfer mentioned in Section IV. A, Equations 9 to 19, characteristic of the current-potential curve for coulopotentiography (i.e., the coulopotentiogram), are studied as follows.

When a reversible electrode, reaction 9, takes place in a column electrode, the decrease of the amount of Ox at the electrode surface is given as in Equation 19. Here, instead of u in Equation 21, a volume (S), height of unit, length, and base area of S are considered. S is the effective cross section of the solution path in the column electrode. Then, the following equation is given by using the total concentration (C_0) of Ox and Red.

$$\frac{dC^*_{ox}}{dt} = \frac{1}{S}\frac{dN_{ox}}{dt} = -\frac{\lambda}{S}\left[\frac{C^*_{ox} - \theta(C_0 - C^*_{ox})}{1 + k\theta}\right] \quad (35)$$

Considering the potential scanning with the rate of $r > 0$ ($V \cdot sec^{-1}$), the relationship between potential E, the flow rate f, the electrolytic time t, and transferring length l for solution within time t can be shown as in Figure 26. The solution that exists at present in the vicinity of point l with potential E was introduced into the column electrode at Sl/f sec before the present time with the potential [E + (rSl/f)] (see Equation 28). The variation of concentration of Ox at time t and at point l′ with potential [E + (rSl/f) - rt] is then given from Equations 20 and 35 as ($0 < t = Sl'/f <$ Sl/f).

$$\frac{dC^*_{ox,t}}{dt} = -\frac{\lambda}{S}\left[\frac{C^*_{ox,t} - (C_0 - C^*_{ox,t})\theta \exp\frac{nF}{RT}r\left(\frac{Sl}{f} - t\right)}{1 + k\theta \exp\frac{nF}{RT}r\left(\frac{Sl}{f} - t\right)}\right] \quad (36)$$

Then, Equation 36 is solved on the simplifying assumption of k = 1 and under the condition of $C^*_{ox} = xC_0$ at t = 0.

$$C^*_{ox,t} = C_0\left\{\left[\frac{\theta A}{1+\theta A} + \frac{SM}{\lambda}\frac{\theta A}{(1+\theta A)^2} + \ldots + \frac{1^{d(n)}\left\{\frac{\theta A}{1+\theta A}\right\}}{\lambda^n\, dt^n}\right] + \left[x - \frac{\theta B}{1+\theta B} - \frac{SM}{\lambda}\frac{\theta B}{(1+\theta B)^2} - \frac{S^2{}'M^2}{\lambda^2}\frac{\theta B(1-\theta B)}{(1+\theta B)^3} - \ldots\right]\exp\left(-\frac{\lambda t}{S}\right)\right\} \quad (37)$$

$$A = \exp\left[\frac{nF}{RT}r\left(\frac{Sl}{f} - t\right)\right] \quad (38)$$

$$B = \exp\left(\frac{nF}{RT}r\frac{Sl}{f}\right) \quad (39)$$

$$M = \frac{nF}{RT}r \quad (40)$$

The current (Δi_l) that flows through the small region (Δl) in the vicinity of point l with potential E is

$$\Delta i_l = -nF\left(\frac{dN_{ox}}{dt}\right)_{t = Sl/f}\Delta l = nFSC_0\,\Delta l\left\{\left[M\frac{\theta}{(1+\theta)^2} + \frac{SM^2}{\lambda}\frac{\theta(1-\theta)}{(1+\theta)^3} + \ldots\right] + \left[\frac{\lambda}{S}\left(x - \frac{\theta B}{1+\theta B}\right) - M\frac{\theta B}{(1+\theta B)^2} - \frac{SM^2}{\lambda}\frac{\theta B(1-\theta B)}{(1+\theta B)^3} - \ldots\right]\exp\left(-\frac{\lambda l}{f}\right)\right\} \quad (41)$$

Finally, the total current (I) that flows through the column electrode of length L is given by:

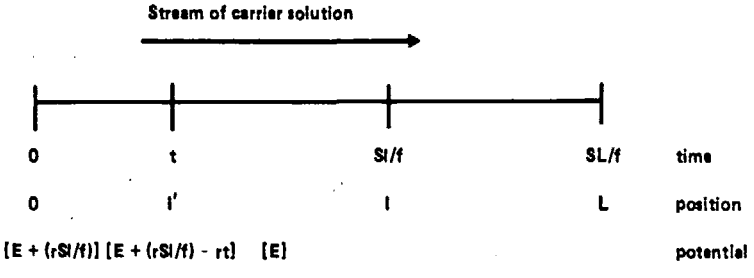

FIGURE 26. Relation between E, f, t, and l.

$$I = \int_0^L \Delta i_l \, dl$$

$$= nFC_o \left\{ xf \left[1 - \exp\left(-\frac{\lambda L}{f}\right)\right] - f\left[\frac{\theta}{1+\theta} - \frac{\theta B}{1+\theta B}\exp\left(-\frac{\lambda L}{f}\right)\right] + Mr\left[\frac{\theta}{(1+\theta)^2}\left(SL - \frac{2Sf}{\lambda}\right)\right. \right.$$

$$\left. + \frac{2Sf}{\lambda}\frac{\theta B}{(1+\theta B)^2}\exp\left(-\frac{\lambda L}{f}\right)\right] + \frac{S}{\lambda}M^2\left[\frac{\theta(1-\theta)}{(1+\theta)^3}\left(SL - \frac{3Sf}{\lambda}\right)\right.$$

$$\left. \left. + \frac{3Sf}{\lambda}\frac{\theta B(1-\theta B)}{(1+\theta S)^3}\exp\left(-\frac{\lambda L}{f}\right)\right] + \ldots\ldots \right\} \quad (42)$$

When $\lambda L/f$ is sufficiently large and electrolytic efficiency $E[= 1 - \exp(-\lambda L/f)]$ is large, Equation 42 becomes

$$I = nFC_o \left\{ xf \left[1 - \exp\left(-\frac{\lambda L}{f}\right)\right] - f\frac{\theta}{1+\theta} + \frac{nF}{RT}r\frac{\theta}{(1+\theta)^2}\left(SL - \frac{2Sf}{\lambda}\right)\right.$$

$$\left. + \frac{1}{\lambda}\left(\frac{nF}{RT}r\right)^2 \frac{\theta(1-\theta)}{(1+\theta)^3}\left(SL - \frac{3Sf}{\lambda}\right) + \ldots\ldots \right\} \quad (43)$$

If the current is controlled by diffusion, the limiting current (I_{dc}) at the cathodic process is given by:

$$\theta = 0 : I_{dc} = nFC_o xf\left[1 - \exp\left(-\frac{\lambda L}{f}\right)\right] \quad (44)$$

and the limiting current (I_{da}) at the anodic process is given by:

$$0 = \infty : I_{da} = nFC_o f(1-x)\left[1 - \exp\left(-\frac{\lambda L}{f}\right)\right] \quad (45)$$

In Equation 43, when r is sufficiently small and/or λ is sufficiently large, higher order terms can be neglected and the equation becomes

$$I = nFC_o \left\{ xf \left[1 - \exp\left(-\frac{\lambda L}{f}\right)\right] - f\frac{\theta}{1+\theta} + \frac{nF}{RT}r\frac{\theta}{(1+\theta)^2}\left(SL - \frac{2Sf}{\lambda}\right) \right\} \quad (46)$$

The coulopotentiogram given by Equation 46 shows a peak current (I_p) proportional to the concentration at the peak potential (E_p), when $r > \frac{fRT}{(SL - 2Sf/\lambda)nF}$.

$$E_p = E_o + \frac{RT}{nF}\ln\left(1 - \frac{2f}{f + \frac{nF}{RT}r\left(SL - \frac{2Sf}{\lambda}\right)}\right) \quad (47)$$

$$\frac{I_p}{I_{dc}} = \frac{1}{1+\theta_p} + \frac{nFr}{RTf}\frac{\theta_p}{(1+\theta_p)^2}\left(SL - \frac{2Sf}{\lambda}\right) \quad (48)$$

$$\theta_p = \exp\left[\frac{nF}{RT}(E_p - E_o)\right] \quad (49)$$

As shown by Equations 44 and 45, the limiting current is directly proportional to the concentration of Ox or Red in sample solution when electrolytic efficiency (E) is large and flow rate (f) is constant (see Equation 34). When r = 0 or very small, the current-potential curve for the coulopotentiography shows the same curves as that for a practical DC polarography.

$$E = E_o + \frac{RT}{nF}\ln\frac{I_{dc} - I}{I - I_{da}} \quad (50)$$

Figure 27 shows coulopotentiograms obtained with a column electrode of large λ value for a reversible electrode reaction, ferrocyanide/ferricyanide system in 1 *M* KCl. From this figure, it is evident that the curve obtained with fast flow rate and slow scan rate has no peak and that with slow flow rate and fast scan rate has a peak as expressed by Equations 45 to 49.

The coulopotentiograms for an irreversible electrode process are shown in Figure 28. Theoretical consideration of the mathematical model, however, is in progress.

B. Continuous Determination of Copper, Lead, and Cadmium by Coulopotentiography[33]

The coulopotentiogram obtained is shown in Figure 29, which was recorded with a solution of 1.0×10^{-4} *M* copper, lead, and cadmium ions in 1 *M* KCl and 0.1 *M* acetic acid under the condition of very slow scan rate, r = 0.0006 V sec^{-1}. As the flow rate (f = 0.000333 1/sec^{-1}) and the limiting current of lead ions measured in the curve was 0.64 mA, the concentration of lead ions can be estimated by the following equation:

$$C = 0.64 \times 10^{-3}/(96500 \times 2 \times 3.33 \times 10^{-4})$$

$$= 9.97 \times 10^{-5} \, M$$

This calculated value agrees well with the true value of 1.00×10^{-4} *M*.

In present coulopotentiography, the amount of electricity consumed in the electrolysis can be estimated by Faraday's law and no calibration

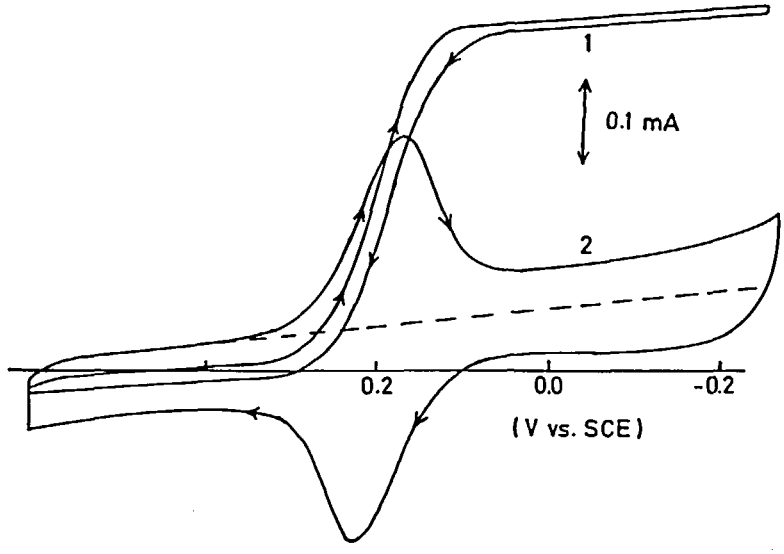

FIGURE 27. Coulopotentiogram for a reversible electrode reaction. Sample: 5 X 10^{-5} *M* $K_3Fe(CN)_6$. Carrier solution: 1 *M* KCl. Flow rate: curve 1, 4.52 ml/min; curve 2, 0.550 ml/min. Scan rate: curve 1, 0.125 V/min; curve 2, 0.500 V/min. Column electrode: two-step column electrode with glassy carbon fiber working electrode of 2 cm (E_t = +0.6 V vs. SCE).

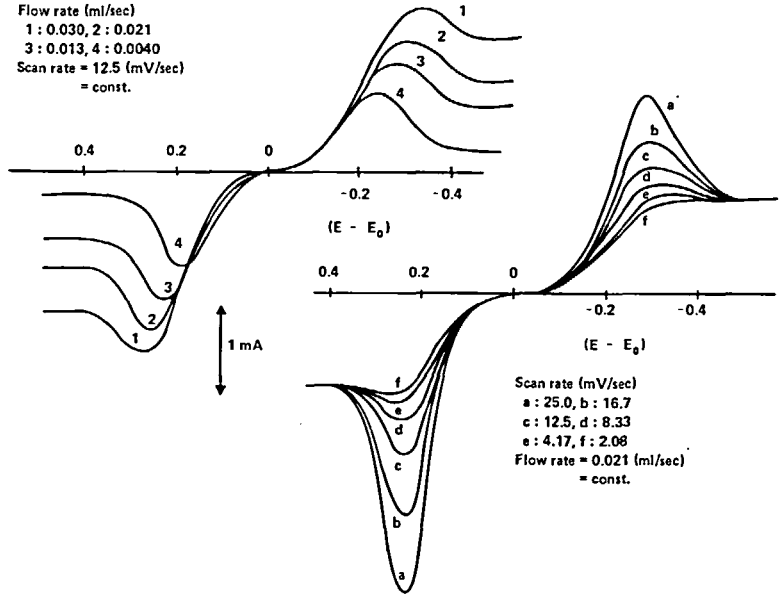

FIGURE 28. Coulopotentiograms for an irreversible electrode reaction. Sample: 10^{-4} *M* iron in 1 *M* H_2SO_4. $k_s = 4.8 \times 10^{-5}$ cm/sec; $\alpha = 0.42$ (cathodic) – both obtained with glassy carbon rotating disk electrode.

curve is necessary. This means that the limiting current is independent of the electrode characteristics as long as the electrode process is fast enough. Moreover, the sensitivity and accuracy are much higher than those of conventional polarography. Therefore, the coulopotentiographic method is valuable in trace analysis of flowing samples. It may be applied to the elucidation of the

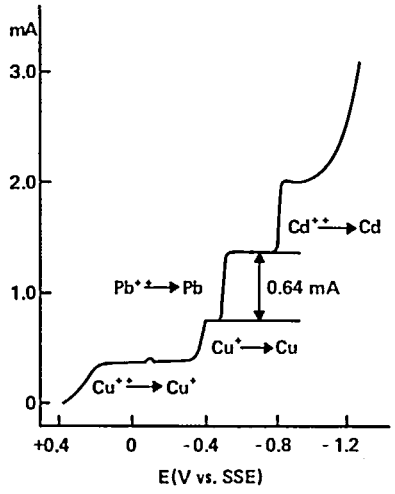

FIGURE 29. Coulopotentiogram of Cu^{2+}, Pb^{2+}, and Cd^{2+}. Sample: 10^{-4} M Cu^{2+}, Pb^{2+}, and Cd^{2+}. Carrier solution: 0.1 M CH_3COOH-1 M KCl. Flow rate: 2.0 ml/min. Scan rate: 0.036 V/min.

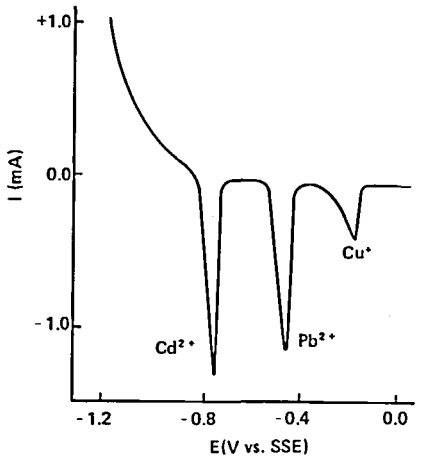

FIGURE 30. Stripping coulopotentiogram of Cu^{2+}, Pb^{2+}, and Cd^{2+}. Sample: 5×10^{-7} mol of Cu^{2+}, Pb^{2+}, and Cd^{2+}. Carrier solution: 0.1 M CH_3COOH-1 M HCl. Flow rate: 2 ml/min. Scan rate: 0.036 V/min.

mechanisms of the electrode reaction and will give fundamental data used for electrolytic chromatography at the column electrode.

VIII. ANODIC STRIPPING COULOPOTENTIOGRAPHY

Although coulopotentiography is a sensitive electrochemical method, due to the scanning of the electrode potential, the background current becomes appreciable when the concentration of the depolarizer decreases as low as 10^{-6} M. Two kinds of stripping coulopotentiography have been developed to eliminate the defects of ordinary coulopotentiography.

A. Stripping Coulopotentiography with Single Cell[33]

As in the case of electrolytic chromatography at uniform electrode potential, the potential of the column electrode is kept at a sufficiently negative potential and all the metallic ions are deposited on the column for a definite period of time; then, the electrode potential is scanned to positive potential by using the same circuit as demonstrated in Figure 25. The dissolution current is recorded against the scanning potential as shown in Figure 30. The anodic stripping coulopotentiogram or the inverse coulopotentiogram was obtained with solutions of 5×10^{-6} M copper, lead, and cadmium ions, which were preelectrolyzed for 50 min at the flow rate of 2 ml/min^{-1}. Then, stripping was carried out at the scan rate of 0.036 V/min^{-1}.

When the sample solution involves both large amounts of soluble ions and small amounts of depositing ions, the simultaneous determination of both ions is possible by using the proposed method as shown in Figure 31.[34] This figure was obtained with a solution of 10^{-6} M copper and 1.5×10^{-4} M iron. The electrode potential was scanned from +0.80 to -0.79 V and stopped for a definite period of time; then, it was scanned again to the positive side. Peak A or the limiting current at the cathodic process indicates the concentration of iron, as mentioned in the preceding chapter; peak B gives the amounts of copper deposited during the concentration time.

The determination was made from the peak area using Faraday's equation or simply from the height of the peak if the scan rate was considerably fast and the electrode reaction proceeded fast enough, as shown in Figure 31, peaks 1, 2, and 3. In this connection, Figures 30 and 31 were obtained by using glassy carbon grain and glassy carbon fiber working electrodes, respectively.

B. Stripping Coulopotentiography with Double Cell[33]

Similar to electrolytic chromatography, the

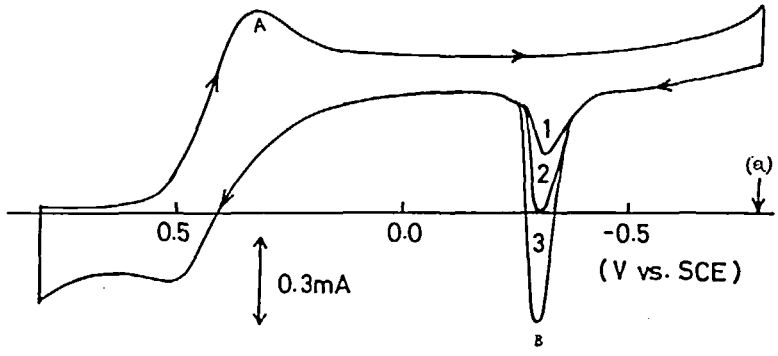

FIGURE 31. Coulopotentiogram of 1.5×10^{-4} *M* Fe^{3+} and 10^{-6} *M* Cu^{2+}. Carrier solution: 0.1 *M* HCl-0.1 *M* KCl. Flow rate: 2.10 ml/min. Scan rate: 0.75 V/min. Waiting time at potential a, −0.79 V; curve 1, 5 min; curve 2, 10 min; curve 3, 20 min.

eluted metal ions are detected at the second cell. Different from electrolytic chromatography, the potential of the first cell (chromatographic cell) is kept at the extremely negative potential for a definite period of time and then scanned to positive potential at a definite rate. The redeposition current at the second cell (detector) is recorded against the potential of the first column electrode. This E_1-I_2 curve again gives the positive coulomb-potential curve as shown in Figure 32.

IX. CONCLUSION

The authors have discussed rapid electrolysis at the column electrode packed with glassy carbon grains or fibers. The column electrode is used not only as the coulometric detector, but also as the chromatographic column for the separation of metals, the concentration of the dilute solutions, the elimination of interfering ions, the elucidation of electrode reaction mechanisms, and the smoothing of the oxidation states. Although the discussion is omitted here, the column cell has been used for the preparation of free radicals in nonaqueous dipolar solvents and similar unstable substances which otherwise cannot be prepared in high concentration. By the use of electrolytic chromatography with coulometric detection, the determination of micro amounts of metals (1 μl or less volume of 10^{-4} *M* sample) is possible, as well as that of trace amounts of metals (10^{-8} *M* or less concentration of several liters) with satisfactory accuracy.

As modifications of coulometry, coulopotentiography and anodic stripping coulopotentiography

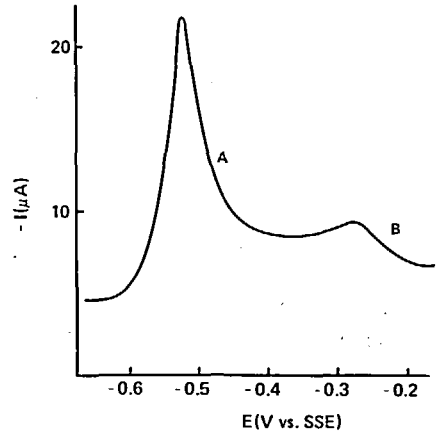

FIGURE 32. Indirect stripping coulopotentiogram of Pb^{2+}. Sample: 250 ml of 1.0×10^{-8} *M* Pb^{2+}. Carrier solution: 0.1 *M* CH_3COOH-1 *M* KCl. Flow rate: 2 ml/min. Scan rate: 0.09 V/min. (Peak B shows trace amounts of copper contained in the carrier solution.)

have been proposed. One of the great advantages of these methodologies is that absolute determinations are possible without preparing any standard for the calibration. Another advantage is the simplicity of the remote control instrumentation. For instance, very dilute lead or cadmium ions in river water can be recorded continuously by the use of electrolytic chromatography: using the two column cells, both of which are kept at the potential of metal deposition, and by a simple switching of the potential of the first cell (E-I) to a dissolution potential with a definite time interval, the record of the current flowed through the

second cell (E-II) indicates the amount of metal concentrated during the interval. The interfering substance, if present, may be removed by the preliminary column cell connected to the first cell.

In this review, two methods have been given, i.e., ordinary electrolytic chromatography and coulopotentiography. In the former, a solution of small volume is introduced into the carrier solution as a sample by a microsyringe; in the latter, the depolarizer in question is contained in the continuously flowing carrier solution. Therefore, electrolytic chromatography is convenient in such experiments for elucidation of electrode reaction mechanisms which require rapid and repetitive procedures and for analysis of samples of small volume or strong radioactivity. This method, however, has disadvantages such as smaller sample size than in the gas chromatographic analysis; that is, though the detection limit is as small as 10^{-9} mol, the lowest determinable limit of concentration is fairly large, 10^{-5} *M*. On the other hand, coulopotentiography has a high sensitivity and, therefore, determination of dilute solution is possible. However, sample volume required is large (more than 50 ml) and the time required to obtain a stationary current is fairly long.

As mentioned above, proposed methods have many methodological possibilities in analytical chemistry and electrochemistry. The authors, however, believe that the following problems should be solved to facilitate further development.

1. Electrode materials. Glassy carbon is expected to be the most practical material for the working electrode from the standpoint of permissible potential range. Nevertheless, further studies on preparations and pretreatments will give more reproducible results.

2. Background currents. As the column electrode has a working electrode of a relatively large surface area, the background current is considerably larger than that of polarography Instrumental or methodological reductions, e.g., stripping methods, should be studied.

3. Other possibilities of the proposed methods. Further studies are desired for instrumental developments such as alternating current superimposed on column electrolysis. On the other hand, applications to the process control or continuous analysis with and/or without other instruments are expected.

ACKNOWLEDGMENT

This research was aided in part by a Scientific Research Grant of the Ministry of Education, Japan. The authors express their sincere thanks to Drs. Setoshi Okazaki and Takeshi Yamada, whose results have been freely used.

REFERENCES

1. Eckfeldt, E. L., *Anal. Chem.*, 31, 1453 (1959).
2. Fujinaga, T., Nagai, T., Takagi, C., and Okazaki, S., *Nippon Kagaku Zasshi*, 84, 941 (1963).
3. Bard, A. J., *Anal. Chem.*, 35, 1125 (1963).
4. Fujinaga, T., Takagi, C., and Okazaki, S., *Kogyo Kagaku Zasshi*, 67, 1798 (1964).
5. Roe, D. K., *Anal. Chem.*, 36, 2371 (1964).
6. Eckfeldt, E. L. and Shaffer, E. W., Jr., *Anal. Chem.*, 36, 2008 (1964).
7. Blaedel, W. J. and Strohl, J. H., *Anal. Chem.*, 36, 1245 (1964).
8. Blaedel, W. J. and Strohl, J. H., *Anal. Chem.*, 37, 64 (1965).
9. Finlayson, M. B. and Mowat, J. A. S., *Electrochem. Technol.*, 3, 148 (1965).
10. Johansson, G., *Talanta*, 12, 163 (1965).
11. Takata, Y. and Muto, G., *Bunseki Kagaku*, 14, 453 (1965); 15, 154 (1966).
12. Okazaki, S., *Rev. Polarogr.*, 15, 269 (1968).
13. Fujinaga, T., Izutsu, K., and Okazaki, S., *Rev. Polarogr.*, 14, 164 (1967).
14. Kihara, S., *J. Electroanal. Chem.*, 45, 31 (1973).
15. Sioda, R. E. and Kambara, T., *J. Electroanal. Chem.*, 38, 51 (1972).
16. Fujinaga, T., *Pure Appl. Chem.*, 25, 709 (1971).

17. Kihara, S., *Bunseki Kagaku,* 22, 1642 (1973).
18. Fujinaga, T., Okazaki, S., and Yamada, T., *Chem. Lett.,* p. 863 (1972).
19. Lingane, J. J., *Anal. Chim. Acta,* 2, 591 (1948).
20. Levich, V. G., *Physicochemical Hydrodynamics,* Prentice-Hall, Englewood Cliffs, New Jersey, 1962.
21. Blaedel, W. J. and Klatt, L. N., *Anal. Chem.,* 38, 879 (1966).
22. Sioda, R. E., *Electrochim. Acta,* 15, 783 (1970).
23. Sioda, R. E., *Electrochim. Acta,* 15, 1559 (1970).
24. Klatt, L. N. and Blaedel, W. J., *Anal. Chem.,* 39, 1065 (1967).
25. Kihara, S., Motojima, K., and Fujinaga, T., *Bunseki Kagaku,* 21, 883 (1972).
26. Kihara, S., Yamamoto, T., Motojima, K., and Fujinaga, T., *Bunseki Kagaku,* 21, 496 (1972).
27. Kihara, S., Yamamoto, T., Motojima, K., and Fujinaga, T., *Talanta,* 19, 657 (1972).
28. Kihara, S., *J. Electroanal. Chem.,* 45, 45 (1973).
29. Kihara, S., Yamamoto, T., Motojima, K., and Fujinaga, T., *Talanta,* 19, 329 (1972).
30. Fujinaga, T., Izutsu, K., Koyama, M., Okazaki, S., and Tsuji, K., *Nippon Kagaku Zasshi,* 89, 673 (1968).
31. Fujinaga, T., Okazaki, S., and Yamada, T., *Chem. Lett.,* p. 863 (1972).
32. Kihara, S. and Fujinaga, T., unpublished.
33. Fujinaga, T., Okazaki, S., and Yamada, T., *Chem. Lett.,* p. 1295 (1973).
34. Kihara, S. and Fujinaga, T., unpublished.